https://doi.org/10.5194/egusphere-2026-4491
Preprint. Discussion started: 24 August 2026

Impact of the variability of O_2 and CO_2 biosphere exchange on modeled O_2-based fossil fuel CO_2 emission estimates

Kim A. P. Faassen[1,2], Auke M. van der Woude[1], Joram J. D. Hooghiem[1], Aleya Kaushik[3,4], Boaz Hilman[5], Wouter Peters[1,6], Penelope A. Pickers[7,8], and Ingrid T. Luijkx[1]

[1]Meteorology and Air Quality, Wageningen University and Research, Wageningen, the Netherlands
[2]Geosciences Research Division, Scripps Institution of Oceanography, University of California, La Jolla, CA, USA
[3]Cooperative Institute for Research in Environmental Sciences, University of Colorado Boulder, Boulder, CO, USA
[4]NOAA Global Monitoring Laboratory, Boulder, CO, USA
[5]Department of Biogeochemical Processes, Max-Planck Institute for Biogeochemistry, Jena, Germany
[6]University of Groningen, Centre for Isotope Research, Energy and Sustainability Research Institute Groningen, Groningen, the Netherlands
[7]Centre for Ocean and Atmospheric Sciences, School of Environmental Sciences, University of East Anglia, Norwich, NR4 7TJ, United Kingdom
[8]National Centre for Atmospheric Science, University of East Anglia, Norwich, NR4 7TJ, United Kingdom

Correspondence: Kim A. P. Faassen (kfaassen@ucsd.edu)

Abstract. Atmospheric oxygen (O_2) can be used to partition components of the carbon budget at global and regional scales. These methods generally assume a constant net biospheric O_2:CO_2 exchange ratio (ER_{net}), although the exchange ratios of the gross fluxes that form ER_{net}, assimilation (ER_a) and respiration (ER_r), vary across ecosystems and time, suggesting ER_{net} may also vary spatially and temporally. To investigate this, we implemented O_2 fluxes in the Simple Biosphere Model (SiB4) by assigning plant functional type- and carbon pool-specific ER_a and ER_r values based on limited observations. This produces the first global O_2 biosphere flux dataset with spatially and temporally varying fluxes (0.5° × 0.5°, 3-hourly). Results show seasonal and spatial variability in ER_{net}, ranging from about 1.1 in winter to 0.8 in summer, with regional summer values differing by more than 0.1 across Europe. Temporal variability is primarily driven by changes in the relative contributions of photosynthesis and respiration, whereas spatial variability reflects differences in dominant plant functional types. The modeled ER_{net} range exceeds the currently recognized terrestrial O_2:CO_2 variability and may effect O_2-based carbon partitioning methods. Neglecting ER_{net} variability can bias regional estimates of fossil fuel CO_2 signals derived from atmospheric potential oxygen. At a strongly biosphere-influenced location, a modeled O_2-derived fossil fuel CO_2 signal of 1.5 ppm is overestimated by nearly 12 ppm when ER_{net} variability is ignored. These results highlight the importance of accounting for biospheric contributions in O_2 partitioning methods.

https://doi.org/10.5194/egusphere-2026-4491
Preprint. Discussion started: 24 August 2026

1 Introduction

Atmospheric oxygen (O_2) can be used to partition the components of the carbon budget at both global and regional scales (Keeling and Manning, 2014; Friedlingstein et al., 2025; Faassen et al., 2023). This is possible because O_2 and carbon dioxide (CO_2) are directly coupled and anti-correlated in two major carbon cycle processes: fossil fuel burning and terrestrial biosphere exchange (Keeling and Manning, 2014). This coupling is quantified by the ratio between the number of moles of O_2 exchanged per mole of CO_2 (Keeling et al., 1998). There are different terms in use to define this ratio depending on the measurement technique and application. When the O_2:CO_2 ratio is based on elemental composition analysis of organic (or fossil) material, the term oxidative ratio (OR) is used and when the O_2:CO_2 ratio is based on direct exchange, the term Exchange Ratio (ER) is used. In this study, we focus on the ER of both gross and net biosphere processes and define the ratio between O_2 and CO_2 exchange as a positive number when the exchange of O_2 and CO_2 is of opposite sign.

The O_2:CO_2 ratio of net terrestrial biosphere exchange (ER_{net}, often indicated as α_B) is generally assumed to be 1.05 $\pm$ 0.1 (Friedlingstein et al., 2025), although other values are also in use, ranging from 1.0-1.2, including the value of 1.1 $\pm$ 0.05 (Severinghaus, 1995) (see Keeling and Manning (2014) for more detail). These values for α_B are based on OR measurements of organic material with the assumption that the ER values of the individual gross fluxes of gross primary productivity (GPP, ER_a) and total ecosystem respiration (TER, ER_r) are equal. The global average O_2:CO_2 of fossil fuel combustion (α_F) is estimated at 1.38, with an uncertainty ranging over time based on the influence of different fossil fuel type with associated α_F uncertainties between 0.03 and 0.07 (Keeling and Manning, 2014).On a global decadal scale, these constant α values are used to partition carbon sinks between the land and the ocean (Friedlingstein et al., 2025), with an uncertainty of 0.1 to the assumed ratio for the biosphere (α_B) which has been shown to be appropriate over these long time scales. This uncertainty is relatively small in comparison to other terms in these large scale O_2 partitioning methods, and on decadal timescales a variability in α_B within the range of 1.05 to 1.10 has minimal impact (Manning and Keeling, 2006; Keeling and Manning, 2014; Rödenbeck et al., 2023).

On regional scales, α_B has been used to determine the contribution of fossil fuel emissions to the observed atmospheric CO_2 signal (Pickers et al., 2022; Rödenbeck et al., 2023) through Atmospheric Potential Oxygen (APO = O_2 + α_B $\times$ CO_2) (Stephens et al., 1998). In these and other similar regional scale O_2-based partitioning methods, the O_2:CO_2 ratio of biosphere-atmosphere exchange has typically also been treated as a constant value (with uncertainties) across space and time, and for all vegetation and soil types. However, spatial and temporal variability in the O_2:CO_2 ratio of biosphere-atmosphere exchange could have implications for the different O_2 partitioning methods in use on regional scale. For example, Rödenbeck et al. (2023) suggested, based on a theoretical calculation, that varying α_B between 1.05 and 1.1 on seasonal timescales increases the uncertainty of estimated fossil fuel emissions using APO substantially in some cases, to the extent that the uncertainty may become comparable to the magnitude of the signal itself. Another example is the observation-based approach by Pickers et al. (2022) to determine changes in regional fossil fuel CO_2 emissions, based on local atmospheric O_2 and CO_2 measurements at

https://doi.org/10.5194/egusphere-2026-4491
Preprint. Discussion started: 24 August 2026

Weybourne in the UK. Their method also uses APO with a constant α_B value in both the background signal and the perturbations from this background signal.

There are relatively few observations available to assess the variability of α_B. Based on OR measurements of organic material, α_B typically falls within a range between 1.0 and 1.1 (Masiello et al., 2008; Keeling and Manning, 2014; Clay and Worrall, 2015; Jürgensen et al., 2021). However, studies measuring ER values based on O_2 and CO_2 exchange of different soil and vegetation types, either in the field or in the laboratory, indicate that the O_2:CO_2 ratio of biospheric fluxes can vary substantially (e.g., Bloom, 2015; Angert et al., 2015; Hilman et al., 2022). The net ER signal of the biosphere (ER_{net}) based on net surface exchange of O_2 and CO_2 results from the contributions of the ER of the assimilation flux (ER_a) and the respiration flux (ER_r), expressed as follows:

$$NEE = -GPP + TER \tag{1}$$

$$-ER_{net} \cdot NEE = ER_a \cdot GPP - ER_r \cdot TER \tag{2}$$

$$ER_{net} = \frac{ER_a \cdot GPP - ER_r \cdot TER}{-NEE} \tag{3}$$

Where NEE is the net ecosystem exchange, GPP is the gross primary productivity and TER is the total ecosystem respiration. In this study, we assume that NEE does not include fires and disturbances and these processes are therefore not included in ER_{net}. Both GPP and TER are defined as positive fluxes and NEE is negative when carbon is taken up at the surface and positive when carbon is released to the atmosphere. We emphasize that ER_{net} is the result of both assimilation and respiration processes, but in itself is a mathematical construct and not related to a single process, as is NEE itself. Therefore, ER_{net} can even become infinite when NEE equals zero (when GPP equals TER, e.g. during the transition from day to night, or from summer to winter). ER_a is challenging to measure *in situ* and there are only limited observations available from a few studies, which show some temporal variability across vegetation types (Seibt et al., 2004; Ishidoya et al., 2013; Bloom, 2015). Similarly, ER_r is also challenging to measure *in situ* with sufficient precision. The few available studies based on soil chamber measurements also show temporal variability and variability among soil types (Seibt et al., 2004; Angert et al., 2015; Ishidoya et al., 2013; Hicks Pries et al., 2020; Hilman et al., 2022). When ER_a and ER_r differ, their values can be used to partition NEE into the gross fluxes of GPP and TER (Ishidoya et al., 2015; Faassen et al., 2023). Moreover, differences between ER_a and ER_r lead to a varying ER_{net} over time as the difference between GPP and TER fluctuates over time. This temporal variability of ER_{net} has been studied in previous work (Ishidoya et al., 2015; Faassen et al., 2023).

To evaluate the consequences of the variability in ER_a and ER_r on the different O_2 partitioning methods, biosphere O_2 fluxes over larger scales are required. Models can help to assess this in the absence of O_2 flux observations. The modeling studies by Huang et al. (2018) and Ding et al. (2022) provided the first global gridded (1.0° x 1.0° resolution) estimates of O_2 biosphere fluxes by linking constant OR values to simulated NEE fluxes from the fifth and sixth coupled model intercomparison project (CMIP5 and CMIP6). Although interesting, this approach misses the influence of vegetation- and soil specific and temporally variable ER_a and ER_r values. Implementing these variable values remains challenging because measurements of these ER's

https://doi.org/10.5194/egusphere-2026-4491
Preprint. Discussion started: 24 August 2026

have only been conducted over relatively short timescales and in a limited number of ecosystems. Furthermore, there is no clear consensus on the drivers of the temporal variability of ER_a and ER_r, making it difficult to even parameterize them in a model. Only a few studies have explicitly incorporated biospheric O_2 fluxes into models by linking ER_a and ER_r separately to gross CO_2 fluxes (Yan et al., 2023; Faassen et al., 2024). However, these studies were limited in scope, covering only specific ecosystems and focusing on diurnal time scales.

With this study, we make a first attempt to link local variability in biosphere ER signals to larger scale O_2 partitioning methods, by integrating O_2 dynamics into the Simple Biosphere model (SiB4) (Haynes et al., 2019). We thereby provide global scale modeled O_2 (and CO_2) biosphere fluxes. Our study does not include validation with observations of O_2 biosphere fluxes due to the limited availability of O_2 flux observations and the current lack of understanding of the drivers of the variability of ER_a and ER_r. Most of the current atmospheric observation sites measuring O_2 only use a single measurement height, which does not allow to derive O_2 fluxes (Faassen et al., 2024), and direct O_2 flux measurements techniques do not yet exist. Therefore, we use our model framework to gain insights into potential consequences for ER_{net} when considering distinct ER_a and ER_r signals. Moreover, we evaluate the theoretical impact of a variable ER_{net} on O_2-based fossil fuel partitioning when applied at atmospheric observational sites for a forest and a coastal site, by using an atmospheric transport model together with our simulated biosphere O_2 and CO_2 fluxes. The simulated O_2 and CO_2 mole fractions allow full or partial reconstructions of APO, ER_{net}, and fossil fuel signals of perturbations of CO_2 mole fractions (ff_{CO_2}) from the background signal.

In this paper, we first describe the O_2 implementation in the SiB4 model (Sect. 2). In Sect. 3 we analyze the resulting O_2 and CO_2 biosphere flux estimates focusing on the temporal and spatial variability of their ratios. We end this section with an evaluation of the sensitivity of the APO partitioning method to a variable ER_{net}, when using our model-derived data in a theoretical framework to estimate CO_2 fossil fuel signals. A detailed discussion of our findings is presented in Sect. 4, where we discuss the potential consequences of our study for different O_2 partitioning methods. Finally, in Sect. 5 we present our conclusions on the temporal and spatial variability of ER_{net} based on our implementation of O_2 into the SiB4 model and its impact on O_2 partitioning methods.

2 Methods

In this section, we describe the setup of the SiB4 model and the implementation of O_2. The O_2 implementation was done for each individual carbon pool. We provide a detailed explanation of our approach to implementing O_2 for each of these pools. Finally, we outline the methodology for the sensitivity study, in which we assess how sensitive our modeled O_2-based fossil fuel partitioning method is to variations in the biosphere ERs. This model-based method is inspired by the observation-based method described by Pickers et al. (2022).

https://doi.org/10.5194/egusphere-2026-4491
Preprint. Discussion started: 24 August 2026

2.1 Terminology used for the ratio between O_2 and CO_2

We integrate information from previous studies that measured O_2 at various parts of the ecosystem, including the atmosphere, the soil and vegetation. These studies do not always define the O_2:CO_2 ratio as the Exchange Ratio (ER), but different terms are used depending on the measurement approach. For simplicity, we use a consistent terminology throughout this study based on the ER. However, it is important to clarify the different terms in use, as we combine results from multiple measurement studies.

The Oxidative Ratio (OR) represents the O_2:CO_2 ratio derived from elemental analysis of organic materials, such as wood or soil samples. OR reflects the stoichiometry of the sampled material and provides an indication of the O_2 and CO_2 exchange required to have formed the material (Randerson et al., 2006; Gallagher et al., 2014; Clay and Worrall, 2015). Consequently, OR represents processes occurring over time scales of years to decades. In contrast, the Exchange Ratio (ER) refers to the O_2:CO_2 ratio that captures the direct O_2 and CO_2 exchange at the time of measurement, reflecting the specific time scale of the measurement period. Atmospheric ER measurements above vegetation can be categorized into ER values based on O_2 and CO_2 mole fraction measurements that are also influenced by other atmospheric processes (ER_{atmos}, (Battle et al., 2019; Faassen et al., 2023, 2024)) or based on surface flux measurements that are a more direct representation of the surface exchange (ER_{net}, Eq. 2) (Seibt et al., 2004; Ishidoya et al., 2013; Faassen et al., 2023). ER_{atmos} represents a mixture of surface and atmospheric processes (Faassen et al., 2024, 2025), and cannot be linked directly to the ER of the biosphere. Instead, ER_{net} measurements should be used. Studies measuring direct O_2 and CO_2 exchange from soils, stems and vegetation often use the inverse of ER (CO_2:O_2). In this case, different terms are used depending on the process being investigated. The Respiration Quotient (RQ) is used for respiration processes (Angert et al., 2015), and the Assimilation Quotient (AQ) is used to study assimilation processes (Cousins and Bloom, 2004; Bloom, 2015; Fischer et al., 2015). In soil studies, the Apparent Respiration Quotient (ARQ) is used when O_2 or CO_2 follow different pathways out of the soil (Angert et al., 2015; Hicks Pries et al., 2020; Hilman et al., 2022). Under such conditions, ARQ provides an approximation of RQ.

In this study, we only use the terms OR and ER. Values for RQ, AQ and ARQ are converted to ER signals, because RQ, AQ and ARQ represent O_2 and CO_2 exchange at the moment of measurement, similar to ER. OR is used when discussing processes over long time scales or referring to the measurements using elemental analysis. OR is frequently associated with the global biosphere ER (α_B), used to partition the global land and ocean carbon sinks (Keeling and Manning, 2014). However, we explore the use of ER values directly for α_B and evaluate the difference between these approaches.

2.2 SiB4 set-up

The O_2 biosphere fluxes are implemented in the Simple Biosphere Version 4 (SiB4) model (Haynes et al., 2019), see Figure 1. Vegetation in the model is categorized into 10 plant function types (PFTs), as summarized in Table 1. The PFTs include different forest types, shrubs, and crops, each forming distinct carbon pools that drive the carbon fluxes. Each carbon pool stores carbon and allocates it to the next pool. Table 1 shows the individual live carbon pools responsible for assimilation and

https://doi.org/10.5194/egusphere-2026-4491
Preprint. Discussion started: 24 August 2026

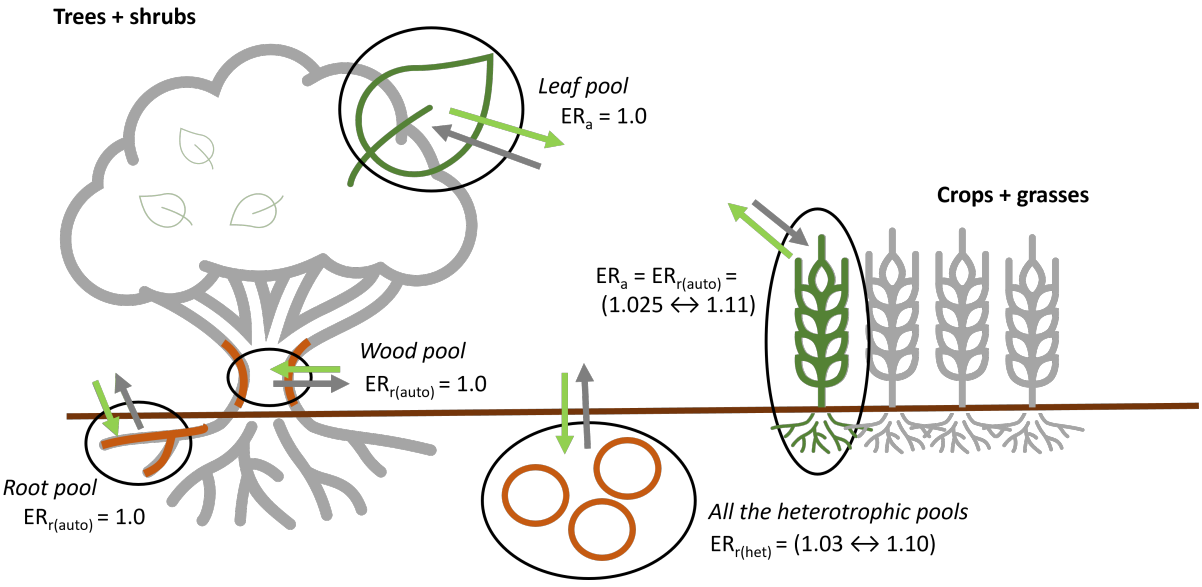

Figure 1. Schematic overview of the different exchange ratios (ER) that are coupled to the carbon pools used in the SiB4 model. ER values are specific for the processes: assimilation (ER_a), autotrophic respiration ($ER_{r(auto)}$) and heterotrophic respiration ($ER_{r(het)}$). The green arrows indicate the O_2 fluxes and the grey arrows indicate the CO_2 fluxes.

autotrophic respiration. For simplicity, we grouped the various dead carbon pools that contribute to heterotrophic respiration into one pool. The size of the autotrophic and heterotrophic flux of each pool for a specific PFT depends on the size of the pool, soil moisture, air temperature and growth of the pool. The different respiration fluxes from the individual pools are added up to get a single respiration flux per PFT type per grid cell.

The SiB4 model calculates surface flux outputs every 10 minutes and we average them to 3-hourly means on a global grid with a resolution of 0.5° by 0.5°. The flux outputs are based on a weighted average of the PFTs within each grid cell. The model uses meteorological data from the ECMWF Reanalysis 5th Generation (ERA5) as input (Hersbach et al., 2020). Consistent with previous studies, the carbon pools were initialized and brought to a steady state using a first-guess quasi-steady-state solution followed by a spin-up of 5 x 20 years with a constant atmospheric CO_2 mole fraction of 370 ppm (Haynes et al., 2019; Kooijmans et al., 2021; Van Der Woude et al., 2023a). This study focuses on the year 2021, a period characterized by relatively normal conditions, such as no extreme drought in Europe and La Niña conditions in the tropics.

2.3 O_2 implementation

Our aim is to generate biosphere O_2 fluxes representative on a seasonal time scale, by using a relatively simple model implementation to assess the implications of spatially and temporally varying ER_{net} by using different values for ER_a and ER_r. For this purpose, we assume that the carbon pool- and PFT-specific ER_a and ER_r values remain constant over time. While

https://doi.org/10.5194/egusphere-2026-4491
Preprint. Discussion started: 24 August 2026

it is highly likely that the ER_a and ER_r values fluctuate due to factors such as light availability (Fischer et al., 2015), vapor pressure deficit, temperature variations, changes in soil moisture (Hicks Pries et al., 2020; Hilman et al., 2022) or vegetation development (Randerson et al., 2006; Gallagher et al., 2014), these dynamics are not accounted for in this study. Instead, we focus only on spatial and temporal variations in the resulting ER signals (ER_{net}, total ER_a and total ER_r) caused by e.g. shifts in dominance of the carbon pools or spatial differences in PFT coverage. This means that we are not looking at the ER variability on the time scale of the SiB4 model output (3-hourly), but rather on a seasonal time scale where ER_r and ER_a could potentially be different values.

The implementation of O_2 into the SiB4 model directly links O_2 fluxes to the CO_2 fluxes for each carbon pool and PFT, using an ER signal depending on the specific carbon pool and PFT:

$$F(O_2)_{pool,PFT} = -ER_{pool,PFT} \cdot F(CO_2)_{pool,PFT} \tag{4}$$

The CO_2 fluxes ($F(CO_2)_{pool,PFT}$) include a GPP flux from the leaf pool, autotrophic respiration fluxes from the leaf, fine roots, coarse roots, wood and product pools (seeds, fruit and flowers) and heterotrophic respiration fluxes from the dead pools. The autotrophic and heterotrophic respiration fluxes can be combined into the TER flux (Eq. 2). Table 1 outlines the ER values used to construct O_2 fluxes from CO_2 fluxes. These values stay constant over time. In the following sections, we provide a detailed reasoning for the selection of ER values for each carbon pool and discuss the specific differences in ER values between grasslands, crops and other PFTs.

Due to the lack of O_2 flux observations and the current limited availability and understanding of ER_a and ER_r measurements, the resulting biospheric O_2 fluxes and its variability are not validated in this study. We discuss this further in Sect. 4. In contrast, the CO_2 biospheric fluxes from the SiB4 model have been validated in previous studies and agree well with observational data (Haynes et al., 2019; Kooijmans et al., 2021; Van Der Woude et al., 2023a).

2.3.1 Leaf and product pool

The ER_a and $ER_{r(auto)}$ values of the leaf pool are both set to 1.0 (Table 1). This is based on the assumption that leaves primarily assimilate and respire glucose, which has an OR of 1.0. Additionally, other carbon-compounds that are being synthesized in leaves (e.g. starch and larger carbohydrates) also have an OR of 1.0 (De Vries et al., 1974; McDermitt and Loomis, 1981). Compounds with an OR differing from carbohydrates, such as lignin, proteins, amino acids, and lipids, are predominantly produced during the growth stage of vegetation (De Vries et al., 1974; Plaxton and Podestá, 2006). Since the current implementation of ER values does not account for growth-stage processes, the production of these compounds is excluded. Previous studies using plant and branch chamber measurements and have found an ER of approximately 1.0 for leaf O_2 and CO_2 exchange (Cousins and Bloom, 2004; Seibt et al., 2004; Ishidoya et al., 2013; Fischer et al., 2015; Gauthier et al., 2018). However, variations in leaf ER may occur depending on the source of nitrogen available to the plant (Cousins and Bloom, 2004; Bloom, 2015) or

https://doi.org/10.5194/egusphere-2026-4491
Preprint. Discussion started: 24 August 2026

Table 1. Implementation of O_2 into the SiB4 model by linking exchange ratio (ER) signals of assimilation (ER_a), autotrophic respiration ($ER_{r(auto)}$ and heterotrophic respiration ($ER_{r(het)}$) to the different carbon pools of specific plant functional types (PFT).

PFT	**ER_a**	**$ER_{r(auto)}$**					**$ER_{r(het)}$**
	Leaf	Leaf	Fine Roots	Coarse Roots	Wood	Product (seeds, fruit and flowers)	All dead pools
Evergreen Needleleaf	1.0	1.0	1.0	1.0	1.0	1.0	1.07[1]
Deciduous Needleleaf	1.0	1.0	1.0	1.0	1.0	1.0	1.08[1]
Evergreen Broadleaf	1.0	1.0	1.0	1.0	1.0	1.0	1.07[1]
Deciduous Broadleaf	1.0	1.0	1.0	1.0	1.0	1.0	1.08[1]
Shrubs	1.0	1.0	1.0	1.0	1.0	1.0	1.10[1]
Tundra	1.0	1.0	1.0	1.0	1.0	1.0	1.10[1]
Grassland	1.025[2]	$=ER_a$	$=ER_a$	$=ER_a$	$=ER_a$	$=ER_a$	1.03[1]
Cropland	1.03[3]	$=ER_a$	$=ER_a$	$=ER_a$	$=ER_a$	$=ER_a$	1.05[1]
Maize	1.03[3]	$=ER_a$	$=ER_a$	$=ER_a$	$=ER_a$	$=ER_a$	1.05[1]
Soybeans	1.11[3]	$=ER_a$	$=ER_a$	$=ER_a$	$=ER_a$	$=ER_a$	1.05[1]
Winter Wheat	1.03[3]	$=ER_a$	$=ER_a$	$=ER_a$	$=ER_a$	$=ER_a$	1.05[1]

1: Clay and Worrall (2015), 2: Randerson et al. (2006), 3: Gallagher et al. (2014)

variation in temperature Bruhn et al. (2025).

The product pool has a minimal impact on respiration fluxes and is difficult to measure. Therefore, we have kept the $ER_{r(auto)}$ for this pool at 1.0 to avoid unnecessary complexity.

2.3.2 Root pool

The $ER_{r(auto)}$ values for both the fine and coarse root pools are set to 1.0 (Table 1), under the assumption that root respiration primarily involves the burning of carbohydrates (Saglio and Pradet, 1980; Hoch et al., 2003; Zhalnina et al., 2018). However, direct measurements of O_2 and CO_2 exchange from both fine and coarse roots show a large range for $ER_{r(auto)}$ with values both above and below 1.0 (Shane et al., 2004; Rachmilevitch et al., 2006; Bathellier et al., 2009; Hicks Pries et al., 2020; Hilman et al., 2021, 2022). This inconsistency challenges the assumption and remains unexplained. One hypothesis is that respiratory substrates other than carbohydrates are utilized. However, studies measuring $\delta^{13}C$ next to O_2 and CO_2 exchange have not found evidence of such changes, supporting the dominance of carbohydrate oxidation (Bowling et al., 2008; Bathellier et al., 2009; Hilman et al., 2021). Other potential explanations for the observed variability include: (1) nitrate assimilation, which reduces ER (Shane et al., 2004; Rachmilevitch et al., 2006); (2) carbon re-fixation within the root system, which increases ER (Bathellier et al., 2009; Hilman et al., 2021); (3) carbon dissolution in xylem water, which also increases ER (Aubrey and

https://doi.org/10.5194/egusphere-2026-4491
Preprint. Discussion started: 24 August 2026

Teskey, 2009); and (4) measurement uncertainty. Given the unexplained nature of the observed ER values in roots, we base our implementation on theoretical assumptions and set the $ER_{r(auto)}$ to 1.0 as an initial approximation.

2.3.3 Wood pool

We set the $ER_{r(auto)}$ value for the wood pool to 1.0 (Table 1), under the theoretical assumption that stem respiration primarily oxidizes carbohydrates (Hoch et al., 2003; Plaxton and Podestá, 2006). However, field measurements report $ER_{r(auto)}$ values exceeding 1.0, with some studies observing values higher than 2.0 (Hilman et al., 2019, 2022; Helm et al., 2023), contradicting the theoretical assumption. Similar to root respiration, the oxidation of alternative substrates, such as lipids, is considered unlikely because of low lipid concentration in woody samples (Hoch et al., 2003) and no indication in ER measurements that lipids are produced before they are oxidized (Hilman et al., 2019). Potential explanations for elevated ER values are similar to those for root respiration: (1) carbon re-fixation within the stem (Hilman et al., 2019); (2) carbon dissolution in xylem water after respiration (Teskey et al., 2008; Hilman et al., 2022) and (3) measurement uncertainty. Despite these hypotheses, no clear consensus has been reached on the mechanisms underlying the observed high $ER_{r(auto)}$ values in stem respiration (Helm et al., 2023). Given this uncertainty, we use an $ER_{r(auto)}$ value of 1.0 for the wood pool as a theoretical baseline.

2.3.4 Heterotrophic respiration pools

For the dead pools, we use a single $ER_{r(het)}$ value for their heterotrophic respiration, which is derived from the OR of the associated plant functional type. The dead pools include: dead biomass, metabolic litter, structural litter, soil litter, and the slow and armored pools. While these individual pools can be conceptually distinguished, direct measurements in bulk soil often make it difficult to determine specific ER values for each of them. Consequently, we grouped them together and assigned a unified ER value for the heterotrophic respiration. The underlying hypothesis is that the ER of bulk soil processes closely reflects the OR of the soil. This is based on the assumption that the compounds contributing to the soil's OR are decomposed during microbial respiration. The smaller and more oxidized compounds are favored, making the soil more reduced over time and increasing the OR above 1. As a result, the ER of heterotrophic respiration has been hypothesized to be higher than that of autotrophic respiration.

This hypothesis is supported by *in situ* measurements that found $ER_{r(het)}$ values consistently exceeding 1.0 (Angert et al., 2015; Hicks Pries et al., 2020; Hilman et al., 2022). These measurements also indicate that $ER_{r(het)}$ remains relatively constant over time except during periods with low respiration rates caused by low temperatures. Under such conditions, $ER_{r(het)}$ values can increase dramatically (exceeding 2.0), as slower processes becomes more apparent, including the oxidation of Fe^{2+} or the higher dissolution of CO_2 into groundwater relative to O_2 (Hicks Pries et al., 2020; Hilman et al., 2022). For the purposes of this study, we neglect this temperature-driven variability and assume a constant $ER_{r(het)}$ over time per PFT. The $ER_{r(het)}$ values of the PFTs are derived from the OR measurements reported by Clay and Worrall (2015) (Table 1).

https://doi.org/10.5194/egusphere-2026-4491
Preprint. Discussion started: 24 August 2026

2.3.5 Crops and grasses

We approach the ER signals of ER_a and $ER_{r(auto)}$ for crops and grasses differently than for the other PFTs. The reason for this choice is that forest types, shrubs and tundra represent relatively slow-growing vegetation compared to crops and grasses which grow faster. Our focus is on the changes in the net ER of the biosphere over a one-year period. This time scale is too short to reliably correlate the OR of slow-growing vegetation with the ER. However, grasses and crops complete their growth within a single year, making it plausible to link their OR to the ER, as hypothesized by Gallagher et al. (2014). By assuming that the OR reflects the net O_2 and CO_2 exchange required to form the complete organic matter of the vegetation (either the grasses or the crops), we propose that ER_a and $ER_{r(auto)}$ should have the same value (Table 1). The OR values for grasses and crops are based on the limited studies that present them: Randerson et al. (2006) for herbaceous plant parts, which we assume are representative values for grass, and Gallagher et al. (2014) for the different types of crops (Table 1). With this implementation we introduce more variability in the resulting O_2 fluxes.

2.4 Fossil fuel sensitivity study

The implementation of O_2 into the SiB4 model offers the opportunity to test the consequence of using a variable ER for the biosphere, both spatially and temporally, for estimating fossil fuel CO_2 signals through atmospheric potential oxygen (APO), as compared to using a constant ER value of 1.1 (α_B = 1.1) (Severinghaus, 1995). We tested the impact of a variable α_B on model-based fossil fuel flux estimates using the tracer APO, an approach that was first proposed by (Pickers et al., 2022). APO is defined as (Stephens et al., 1998):

$$APO = \overbrace{O_2}^{\mathrm{TotalO_2}} - \alpha_B \cdot \overbrace{CO_2}^{\mathrm{TotalCO_2}} \tag{5}$$

The total atmospheric mole fraction signals of O_2 and CO_2 include the following processes: fossil fuel combustion (ff), biosphere exchange (bio), ocean uptake and outgassing and background signals, i.e. the accumulated CO_2 in the atmosphere from all historical exchange with fossil, terrestrial, and oceanic reservoirs. Pickers et al. (2022) used the following definition of APO to calculate CO_2 fossil fuel fluxes based on O_2:

$$ff_{CO_2}[APO] = \frac{APO - APO_{BL}}{\alpha_F - \alpha_B} \tag{6}$$

Where α_F is the oxidative ratio of fossil fuel combustion and corresponds to $ff_{O_2} = \alpha_F \cdot ff_{CO_2}$, and APO_{BL} is the APO baseline, which mainly represents changes due to the ocean processes of both O_2 and CO_2, as well as the background value of O_2. Pickers et al. (2022) estimated APO_{BL} by curve fitting the seasonal variations of APO of atmospheric measurements.

For the purpose of this study, we focus solely on the effect of not taking into account the variability of α_B in Eq. 6 on the estimated ff_{CO_2}[APO]. As a result, ocean fluxes and background values are not of importance for our analysis and are therefore not included, which is different compared to the observation-based study by Pickers et al. (2022). Incorporating ocean and background signals in our model would introduce the same terms that we would subsequently remove, which works because

https://doi.org/10.5194/egusphere-2026-4491
Preprint. Discussion started: 24 August 2026

we use a model-based approach. Consequently, we are able to exclude APO_{BL} from the equation. Without accounting for oceanic processes and background contributions, we can rewrite Eq. 5 into a new version:

$$APO_{wo} = \overbrace{ff_{O_2} + bio_{O_2}}^{\text{TotalO}_2} - \alpha_B \cdot \overbrace{ff_{CO_2} + bio_{CO_2}}^{\text{TotalCO}_2} \tag{7}$$

Where APO_{wo} is APO without ocean and the background signal and it represents the original APO through: $APO_{wo} = APO - APO_{BL}$. APO_{wo} can then be used to estimate the perturbations from the complete background signal, caused by fossil fuel emissions ($ff_{\text{CO}_2}[APO]$):

$$ff_{CO_2}[APO] = \frac{APO_{wo}}{\alpha_F - \alpha_B} \tag{8}$$

To simulate a $ff_{\text{CO}_2}[APO]$ signal, we used the regional atmospheric Stochastic Time-Inverted Lagrangian model (STILT) (Gerbig et al., 2003; Lin et al., 2003). STILT simulates the transport of fossil fuel and biosphere O_2 and CO_2 fluxes, generating a 3-hourly atmospheric signal that can be used to calculate a simulated APO_{wo} signal. STILT uses ECMWF-IFS meteorological fields to calculate the footprint from a receptor location with a resolution of 0.1° by 0.2° (Roberts et al., 2018). At this receptor location, 250 particles are released and followed through the meteorological fields backwards in time for 10 days, until they are exchanged with the surface or go outside the domain, similar to the approach described by Van Der Woude et al. (2023a). Our domain in this study is Europe (15°W - 35°E; 33°N - 72°N) and any signal from outside the domain together with the background signal is considered to be non-local background. The footprint of the receptor locations determines which biospheric and fossil fuel surface fluxes are taken into account. The biosphere fluxes from the SiB4 model are used, together with fossil fuel fluxes from the GridFED dataset (Steinbach et al., 2011; Jones et al., 2021). GridFED categorizes fossil fuel emissions into four types, each with a specific OR: coal (OR = 1.17), oil (OR = 1.44), natural gas (OR = 1.95) and cement (OR = 0, indicating no O_2 uptake).

The resulting simulated atmospheric O_2 and CO_2 signals were analyzed at two stations: Weybourne (WAO, at 15 m height above the surface), a coastal station in a rural part of the United Kingdom (Adcock et al., 2023; Pickers et al., 2022), and Białystok (BIK, at 300 m height above the surface), a station in Poland mostly influenced by biosphere fluxes (Popa et al., 2010). Figure A1 in the appendix shows the yearly sum of the footprint influence for both stations, based on STILT. APO_{wo} was calculated for both stations using the transported fossil fuel and biosphere surface fluxes, together with the α_B based on the transported biosphere fluxes and α_F based on the transported fossil fuel fluxes within these footprints. To assess the impact of using a constant value for α_B instead of the biosphere O_2 and CO_2 flux ratios provided by the SiB4 model, APO_{wo} was also calculated using a fixed value of 1.1 for α_B. The difference in ff_{CO_2}[APO] between the two methods offers insight into the significance of accounting for a variable α_B both over time and space.

To simulate the complete atmospheric signal at WAO and BIK, the non-local signal of the biosphere and fossil fuel combustion originating from outside the European domain, together with the ocean exchange, have to be combined with the local signal from withing the European domain. To achieve this, we have used the global chemistry Transport Model version 5 (TM5)

https://doi.org/10.5194/egusphere-2026-4491
Preprint. Discussion started: 24 August 2026

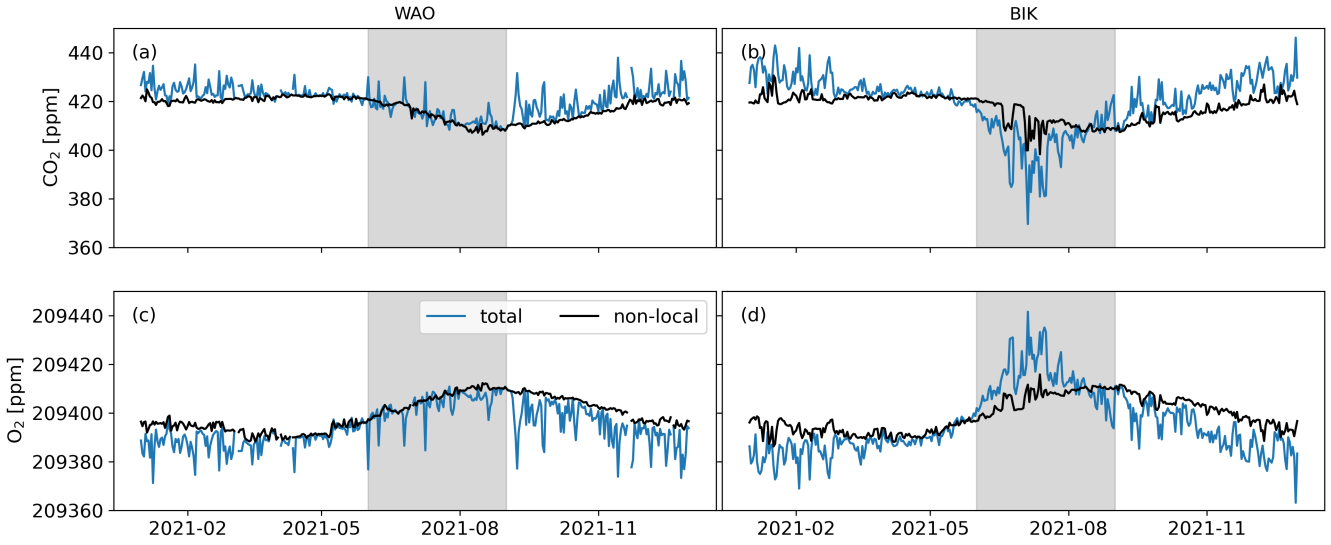

Figure 2. Time series of the simulated mole fractions that result from transported surface fluxes by STILT for Weybourne (left column, WAO) and Białystok (right column, BIK) for CO_2 (a-b) and O_2 (c-d). The non-local signal is the result of TM5 simulations and consists of global mole fractions resulting from fluxes from outside the European domain together with the background signal and transported by STILT from the boundaries of the domain to the two locations. The total signal includes both the non-local signal and the fluxes from the footprint inside the European domain, transported by STILT. The grey shading indicates the summer period between 2021-06-01 and 2021-09-01.

(Krol et al., 2005). TM5 is an Eulerian atmospheric transport model that was run on a 1° by 1° grid and, like the SiB4 model, using ERA5 meteorological data as input. The surface fluxes from SiB4 and GridFED were used to generate the biological and fossil fuel signals, respectively. Additionally, ocean fluxes from the Community Earth System Model (CESM) (Yeager et al., 2022) and a background concentration were included. By transporting both the non-local signal from TM5 and the local signal resulting from surface fluxes within the footprint using STILT, we reconstructed the total atmospheric signal at the receptor location (Figure 2). The modeled seasonal cycles of atmospheric CO_2 and O_2 exhibit amplitudes that are of similar magnitudes as observations at the measurement stations (Adcock et al., 2023; Popa et al., 2010). In this study, we focus exclusively on the local signal (or the perturbations from the background), defined as the total signal minus the non-local contribution from outside our domain.

We analyze the difference between the fossil fuel atmospheric signal obtained with APO using either a value for α_B of 1.1 ($ff_{CO_2}[APO_{(\alpha_B = 1.1)}]$) or using the variable α_B values from SiB4 (ff_{CO_2}[true]). We focus on individual days to compare the derived ff_{CO_2} with the original CO_2 fossil fuel emissions used in the model (from GridFED). These are the CO_2 fossil fuel emissions of ff_{CO_2}[true] and can be linked to the atmospheric fossil fuel signal by:

$$ff_{CO_2}[true] = \sum (FI \cdot F(ff_{CO_2})_s[true]) \quad (9)$$

https://doi.org/10.5194/egusphere-2026-4491
Preprint. Discussion started: 24 August 2026

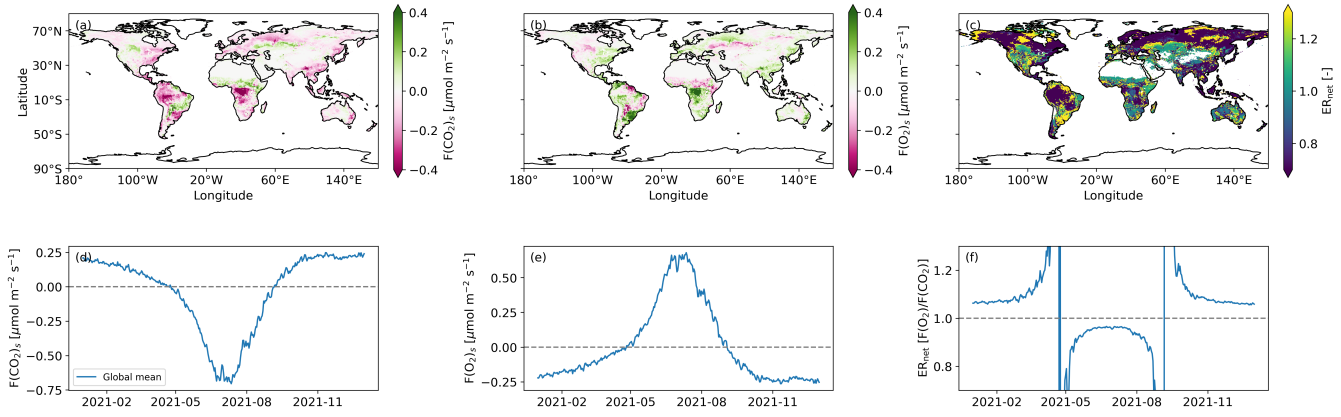

Figure 3. SiB4 model results for the year 2021 including the net CO_2 flux (a), net O_2 flux (b) and their exchange ratio (ER, c), together with the corresponding globally averaged time series over 2021 (d-f).

Where FI is the footprint influence in ppm (μmol m^{-2} s^{-1})$^{-1}$, $F(ff_{CO_2})_s[true]$ is the surface flux of the CO_2 fossil fuel emissions (in μmol m^{-2} s^{-1}) and $ff_{CO_2}[true]$ is the atmospheric fossil fuel signal in ppm. For the atmospheric signal of $ff_{CO_2}[APO_{(\alpha_B = 1.1)}]$, the footprint stays the same. However, the fossil fuel fluxes that would have formed this signal ($F(ff_{CO_2})_s[APO_{(\alpha_B = 1.1)}]$) are now modified:

$$ff_{CO_2}[APO_{(\alpha_B=1.1)}] = \sum(FI \cdot F(ff_{CO_2})_s[APO_{(\alpha_B=1.1)}]) \tag{10}$$

To calculate the $F(ff_{CO_2})_s[APO_{(\alpha_B = 1.1)}]$ surface fluxes, the ratio between the atmospheric signal of $ff_{CO_2}[APO_{(\alpha_B = 1.1)}]$ and $ff_{CO_2}[true]$ can be used:

$$F(ff_{CO_2})_s[APO_{(\alpha_B=1.1)}] = \frac{ff_{CO_2}[APO_{(\alpha_B=1.1)}]}{ff_{CO_2}[true]} \cdot F(ff_{CO_2})_s[true] \tag{11}$$

With Eq. 11 the effect of using a constant α_B of 1.1 on fossil fuel emission estimates can be quantified.

3 Results

In this section we present the results of incorporating O_2 into the SiB4 model. We begin by examining the O_2 and CO_2 fluxes averaged over 2021 for the entire globe (Section 3.1). To gain better insights into the behavior of the resulting ER signal from these fluxes, we furthermore focus on Europe and analyze seasonal variations. Our analysis shows that the ER_{net} signal exhibits distinct temporal and spatial patterns, and we discuss the underlying drivers of these patterns. Finally, we assess the effect of using a variable α_B on the APO method used to estimate fossil fuel emissions (Section 3.2).

https://doi.org/10.5194/egusphere-2026-4491
Preprint. Discussion started: 24 August 2026

3.1 Spatial and temporal variability of ER_{net}

Global biospheric O_2 fluxes exhibit both large spatial and large temporal variability, with elevated O_2 fluxes found in tropical regions and during the summer months. The choices made for the implementation of O_2 into the model are evident from the strong anti-correlation between O_2 and CO_2 fluxes, as shown in Figure 3a and 3b. Using the O_2 and CO_2 fluxes, we calculated ER_{net} signals for the entire globe. However, it is challenging to represent the biospheric ER_{net} with a single averaged value for the entire world. At first glance, the anti-correlated O_2 and CO_2 fluxes appear similar. However, when their ratios are calculated, the resulting ER_{net} signals reveal differences both temporally (Figure 3f) and spatially (Figure 3c), including the aforementioned asymptotic values when NEE ≈ 0.0 μmol m^{-2} s^{-1} in spring and fall (see eq. 2). Globally, ER_{net} fluctuates above 1.0 during the Northern Hemisphere (NH) winter and below 1.0 in the NH summer. By dividing the globally averaged O_2 flux by the globally averaged CO_2 flux for 2021, a single global ER_{net} value is obtained: 0.42. This low global ER_{net} value can be explained by its spatial pattern, which shows extremely low ER_{net} values in tropical and boreal regions (below 0.7 or even lower than 0.0). These extremely low ER_{net} values cannot be directly linked to any of the implemented ER_a or ER_r values (Table 1), and cannot be used for global scale land and ocean sink partitioning. To fully understand the global ER_{net} patterns, we have to look at the individual gross processes that form the ER_{net}.

The ratio between the gross fluxes of GPP and TER can lead to extreme values of ER_{net}. The extreme values of ER_{net} can be explained by reformulating Eq. 2 to:

$$ER_{net} = \frac{ER_a \cdot \frac{GPP}{TER} - ER_r}{\frac{GPP}{TER} - 1} \tag{12}$$

From this equation it becomes evident that ER_{net} depends on three primary variables: ER_a, ER_r and the GPP/TER ratio. In contrast to the global ER_{net} values (Figure 3c), the global values for ER_a (Figure 4a) and ER_r (Figure 4b) remain within the expected ranges prescribed in Table 1 and exhibit only a small annual cycle, caused by changes in PFT dominance (Figure 4d and 4e). The globally averaged GPP/TER ratios are close to 1.0 (Figure 4c), showing that the modeled biosphere is approximately in a steady state if one integrates over long time periods. As indicated by Eq. 12, when the GPP/TER ratio approaches 1.0, ER_{net} can experience extreme values. This relationship becomes apparent when comparing the global time series of GPP/TER (Figure 4f) with ER_{net} (Figure 3f), where ER_{net} shows asymptotic values when GPP/TER crosses 1.0 (GPP = TER, and NEE ≈ 0.0 μmol m^{-2} s^{-1}). Consequently, ER_{net} is not linked to a single biological process, but is a mathematical combination of the individual gross fluxes, showing unexpected values, similar to isofluxes of $\delta^{13}C$ or $\delta^{18}O$ analyses (Miller and Tans, 2003). To further investigate ER_{net}, we focus on regional dynamics in Europe.

ER_{net} in Europe exhibits distinct temporal and spatial patterns, with each season characterized by unique features (Figure 5). During the winter months (December - February, DJF), ER_{net} shows minimal spatial variation across Europe (Figure 5a). In spring (March - May, MAM), ER_{net} values become extreme reflecting dynamic changes in ecosystem processes and NEE values close to zero (Figure 5b). Summer (June - August, JJA) is characterized by low ER_{net} values compared to winter, with a

https://doi.org/10.5194/egusphere-2026-4491
Preprint. Discussion started: 24 August 2026

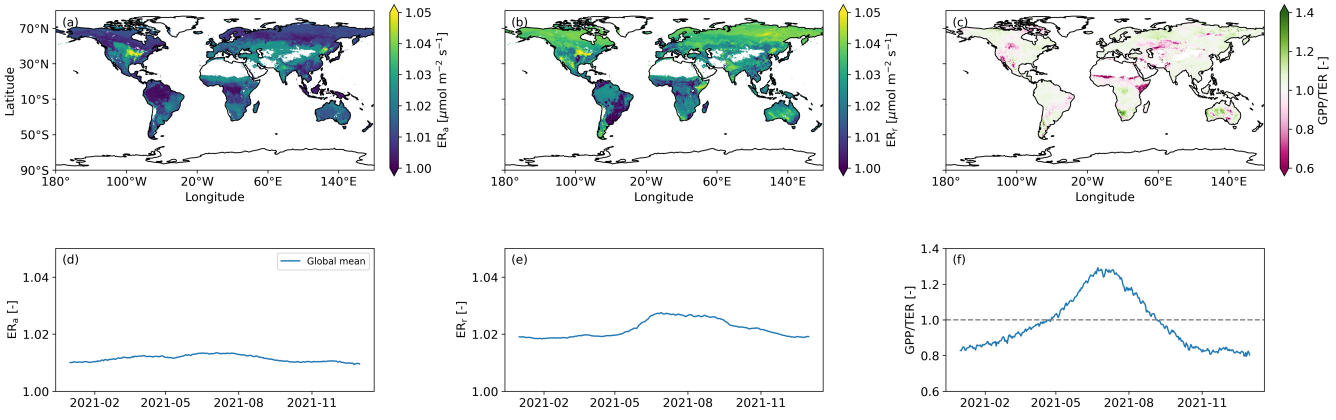

Figure 4. SiB4 model results for the year 2021 for the exchange ratio of assimilation (ER_a) (a), exchange ratio of respiration (ER_r) (b) and the ratio between gross primary productivity (GPP) and total ecosystem respiration (TER) (c), together with the corresponding globally averaged time series over 2021 (d-f).

clear gradient from lower values in the north to higher values in the south (Figure 5c). By fall (September - November, SON) ER_{net} returns to values closer to those found in winter (Figure 5d). As with the global analysis, the seasonal and spatial patterns of ER_{net} can be explained using Eq. 12, highlighting the role of variations in ER_a, ER_r and the GPP/TER ratio in driving these dynamics.

The temporal variation in ER_{net} can be attributed to changes in the GPP/TER ratio (Figures 5e-h). The variability of the GPP/TER ratio depends on environmental changes, such as temperature, amount of light and soil moisture, which creates a clear seasonal pattern. During winter, TER dominates with minimal influence of GPP. According to Eq. 12, when TER is the dominant flux, ER_{net} should approach ER_r (around 1.04), as confirmed by Figure 5. In spring, the GPP/TER ratio approaches 1.0, resulting in extreme ER_{net} values, comparable to the behavior shown in Figure 3 for the global scale. During summer, GPP becomes the dominant flux, but TER remains significant. Eq. 12 suggests that when the GPP/TER ratio is around 1.5, the resulting ER_{net} lies slightly below ER_a (below 1.0). The summer ER_{net} values depend on all components of Eq. 12, including ER_a, ER_r and the individual gross fluxes.

The spatial variations in ER_a and ER_r explain the found spatial variation in ER_{net} during summer. While both ER_a (Figures 5i-l) and ER_r (Figures 5m-p) exhibit less pronounced seasonal variation compared to the GPP/TER ratio, they both display distinct spatial patterns. In particular, a clear north-south gradient is visible during summer, similar to the spatial variation in ER_{net}. In northern Europe (between 60°N and 80°N), ER_a is relatively low and ER_r is relatively high, leading to a low ER_{net} value. In contrast, in southern Europe (between 30°N and 60°N) ER_a is relatively high and ER_r is relatively low, resulting in higher ER_{net} values. These spatial patterns are consistent with the relationships described by Eq. 12.

https://doi.org/10.5194/egusphere-2026-4491
Preprint. Discussion started: 24 August 2026

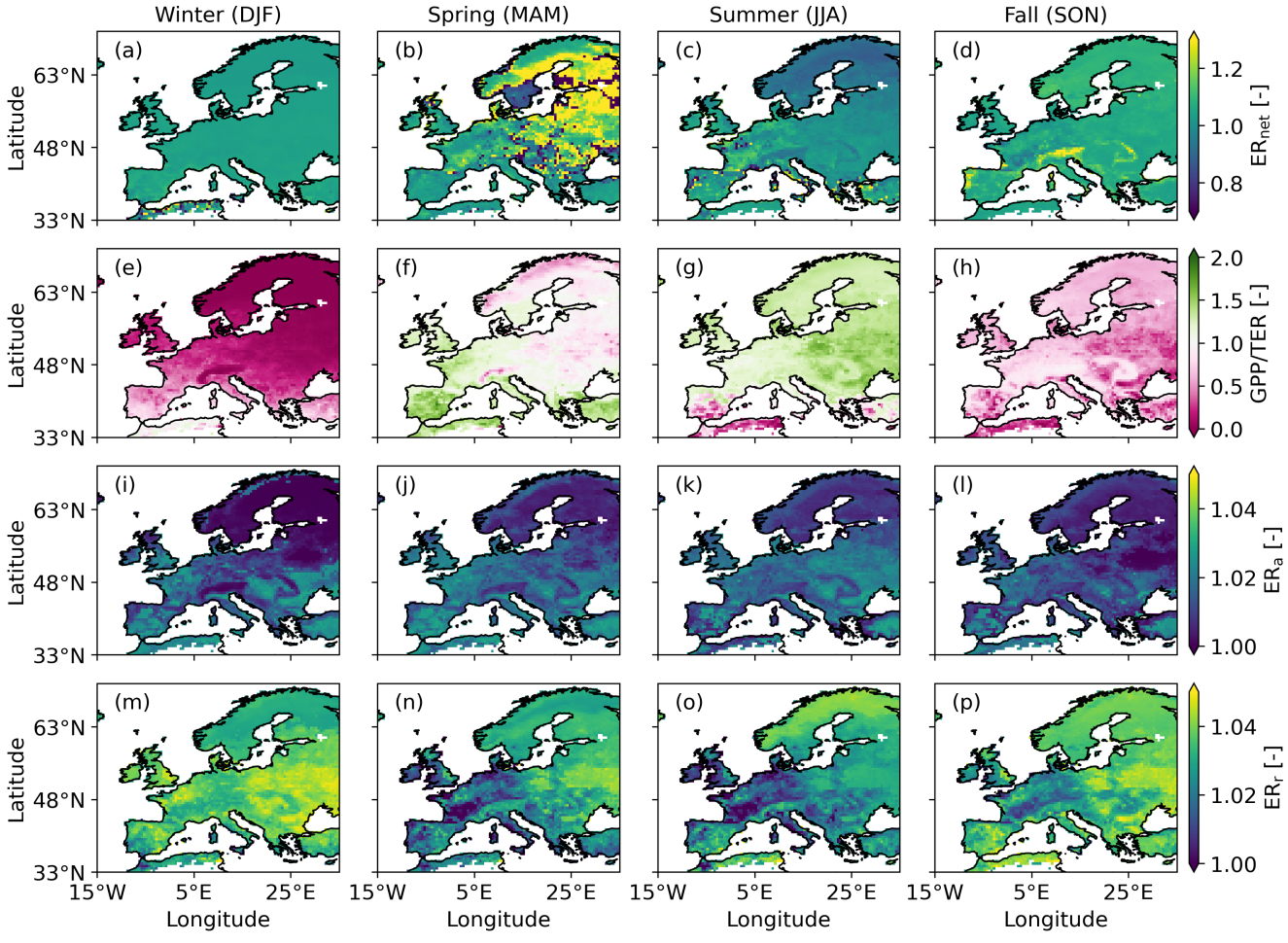

Figure 5. Averaged values of the SiB4 model results during the seasons (from left to right column): winter (December - February, DJF), spring (March - May, MAM), summer (June - August, JJA) and fall (September - November, SON) for the variables (from top to bottom row): the net Exchange Ratio (ER_{net}, a-d), the ratio between gross primary productivity (GPP) and total ecosystem respiration (TER) (e-h), the Exchange Ratio of assimilation (ER_a, i-l) and the Exchange Ratio of respiration (ER_r, m-p).

The spatial variation in ER_a and ER_r is driven by differences in the dominant PFTs. Following our implementation of O_2 in SiB4, variations in ER_a arise from the influence of grasses and crops, while variations in ER_r can result from either crop influence or the relative contributions of autotrophic and heterotrophic respiration (Table 1). The dominant influence is determined by the dominance of the gross fluxes associated with individual PFTs, which are combined in a weighted average net flux. During summer, a clear difference in the contributions of crops and heterotrophic respiration is evident between northern and southern Europe (Figure 6). Crops are more dominant in the south, leading to increased ER_a values. In the north, the more dominant role of trees increases $ER_{r(het)}$ and additionally a more dominant heterotrophic flux increases the ER_r further. The

https://doi.org/10.5194/egusphere-2026-4491
Preprint. Discussion started: 24 August 2026

more dominant heterotrophic flux in the north can again be explained by the less dominant role of grasses and crops, which have a relatively high autotrophic respiration flux in the summer due to their fast growing cycle (Suleau et al., 2011). The GPP/TER ratio does not show a significant difference between northern and southern Europe.

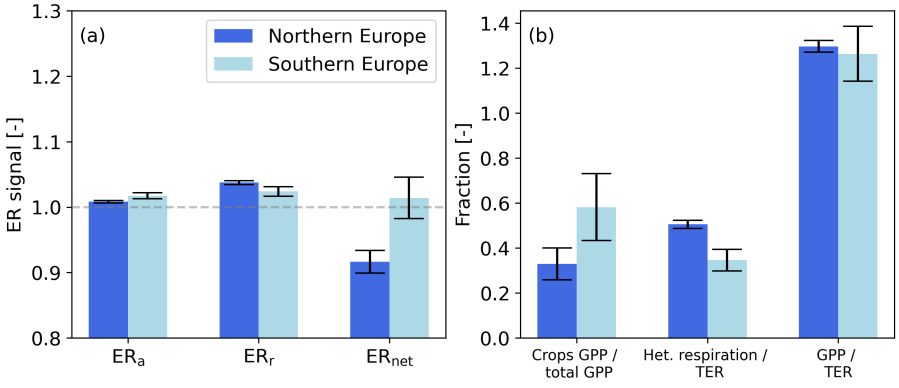

Figure 6. The median values and their median absolute deviation (shown as error bars) for different variables compared between the northern (between 60°N and 80°N) and southern (between 30°N and 60°N) part of Europe during summer 2021 for the: (a) exchange ratios of assimilation (ER_a), respiration (ER_r) and the net fluxes (ER_{net}) and (b) for the ratio between the gross primary productivity (GPP) of crops versus total GPP, the ratio between heterotrophic respiration (Het. respiration) and total ecosystem respiration (TER), and the ratio between GPP and TER.

Overall, the spatial and temporal variability of ER_{net} is primarily determined by the gross fluxes, suggesting that similar variability can be expected for real-world ecosystems. Temporal variability in ER_{net} arises from fluctuations in the ratio between GPP and TER, while spatial variability is driven by the dominance of the gross fluxes of specific PFTs. Although the individual ER values from Table 1 and the biospheric O_2 fluxes have not been validated with observations, the gross CO_2 fluxes simulated by the model are known to be realistic. Previous studies have demonstrated that the spatial and temporal patterns of these CO_2 fluxes and their anomalies align well with observations (Haynes et al., 2019; Smith et al., 2020; Kooijmans et al., 2021; Van Der Woude et al., 2023b). Spatial and temporal variability of ER_{net} is therefore likely because it is driven by the gross CO_2 fluxes. However, the absolute values of ER_{net} still require validation to confirm their accuracy.

To assess the implications of a variable ER_{net} value on O_2 partitioning methods, the simulated ER_{net} values have to be transported into the atmosphere. This is crucial because ER_{net} values associated with a low NEE flux are of less importance compared to ER_{net} values linked with a high NEE flux, as we demonstrate next.

https://doi.org/10.5194/egusphere-2026-4491
Preprint. Discussion started: 24 August 2026

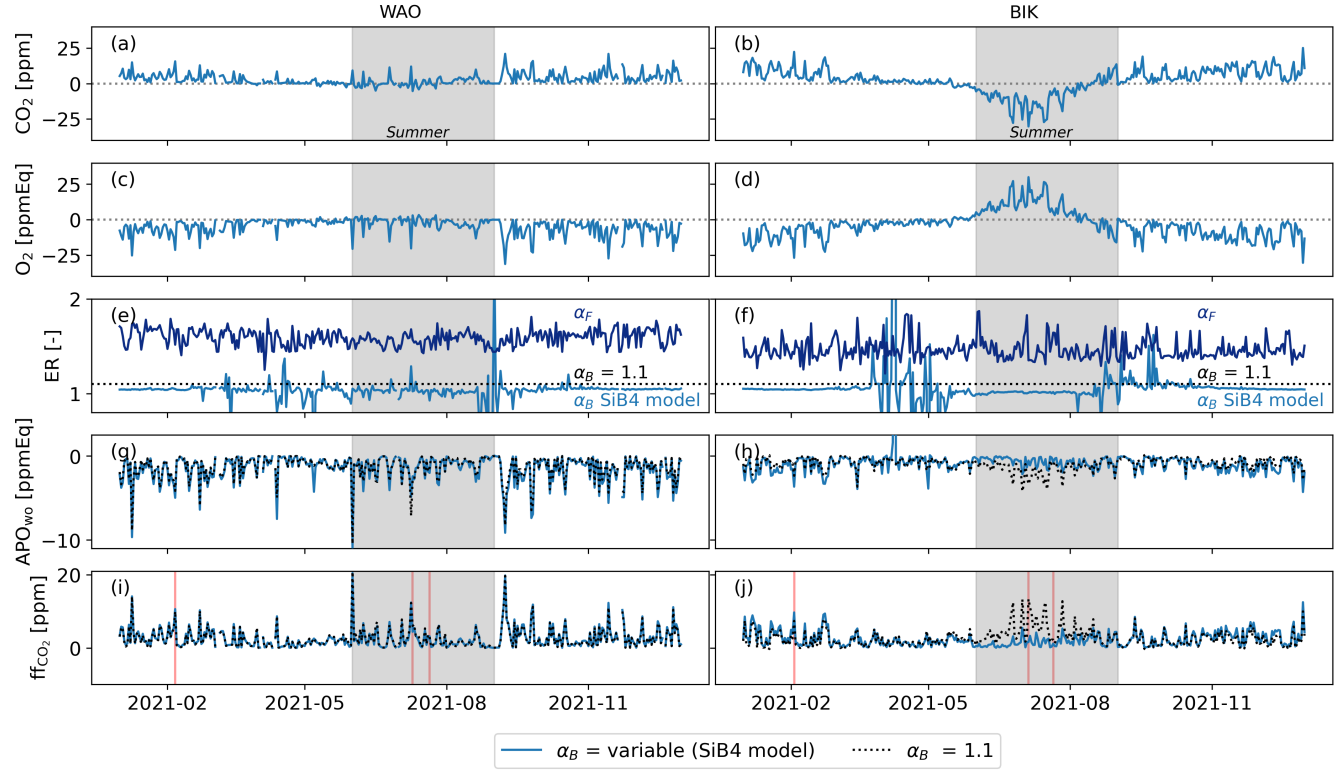

Figure 7. Time series of the transported surface fluxes by STILT for Weybourne, UK (left column, WAO) and Białystok, Poland (right column, BIK) for simulated CO_2 (a-b) and O_2 (c-d) mole fractions, exchange ratios (ER, e-f), atmospheric potential oxygen without ocean and the background signal (APO_{wo}, g-h) and the fossil fuel signal of CO_2 (ff_{CO_2}, i-j). The grey shading indicates the summer period between 2021-06-01 and 2021-09-01. The red vertical lines indicate the three days chosen to analyze the surface fluxes (Figure A3).

3.2 Application of the fossil fuel partitioning method

We confirm that fossil fuel CO_2 signals (ff_{CO_2}) can be calculated correctly from APO when the correct α_B is used in both the numerator and denominator of Eq 8. This true α_B value is obtained with our modeled O_2 and CO_2 surface fluxes from SiB4 by transporting them, along with the GridFED fossil fuel fluxes, to the generate a local signal at two locations using STILT (Figure 7c and 7d). This gave us the temporal variability of both α_B and α_F for WAO and BIK as shown in Figure 7e and 7f, to use in Eq 8. With all components of Eqs. 7 and 8 transported to WAO and BIK, the APO_{wo} signal (Figure 7g and 7h) and ff_{CO_2}[APO] (Figure 7i and 7j) are calculated. We subsequently confirmed that these values of ff_{CO_2}[APO] are exactly equal to the CO_2 signal resulting from transported fossil fuel fluxes (ff_{CO_2}[true], not shown). The APO method worked in this regional case because the variability of both α_B and α_F were taken into account when calculating APO_{wo}. For WAO, our modeled α_B fluctuates around 1.04, with a daily averaged α_B in the winter of 1.04 and in the summer of 1.03. For BIK, the modeled α_B has a daily averaged α_B around 1.04 during winter and around 1.01 in summer. WAO has a higher α_B compared to BIK because it

https://doi.org/10.5194/egusphere-2026-4491
Preprint. Discussion started: 24 August 2026

is situated in an area with a higher contribution from crops and a lower contribution from heterotrophic respiration (Figure 5c). In our analysis, we assume α_F to be accurately known, using GridFED. This α_F also exhibits temporal variability but does not have a clear seasonal cycle at either WAO or BIK. For WAO, α_F fluctuates around 1.6 and for BIK around 1.5.

The definition of APO generally uses a constant value for α_B of 1.1 (or 1.05, or 1.07), based on OR measurements representing long-term terrestrial biosphere exchange (decadal). Using APO with a constant α_B to estimate the fossil fuel influence would only work when the transported biosphere fluxes have the same value for ER_{net} (1.05, 1.07 or 1.1). If we would have implemented O_2 into the SiB4 model with a constant ER (or OR) value (e.g. of 1.1), the resulting transported α_B would also have been a constant value of 1.1 over space and time. In that case, using a constant α_B of 1.1 in Eq. 7 and 8 would again produce the same results for which ff_{CO_2}[APO] compared to the true transported fossil fuel fluxes (ff_{CO_2}[true]). However, as we showed in Sect. 3.1, it is unlikely that the ER of the biosphere is constant on short time scales (daily to seasonal) because of differences between ER_a and ER_r. Therefore, we investigate the implications of assuming a constant α_B of 1.1 in reconstructing ff_{CO_2}[APO], while the transported biosphere fluxes have a variable α_B over time.

We find that CO_2 fossil fuel mole fraction signals derived using APO are overestimated in summertime and underestimated in wintertime, when a constant α_B of 1.1 is applied instead of variable α_B values calculated from the transported biosphere fluxes from the SiB4 model. A constant value for α_B of 1.1 is often higher compared to the 'true' transported α_B (Figure 7e and 7f). This overestimation leads to too negative APO values during summer (Figure 7h and Eq. 6) and consequently, ff_{CO_2}[APO] is also overestimated in summertime (Figure 7j). Overestimating α_B has a larger effect when the biosphere influence is higher (Figure A3 in the appendix). As a result, the difference between $ff_{CO_2}[APO_{(\alpha_B = 1.1)}]$ and ff_{CO_2}[true] is largest at BIK, because BIK is located in a region with forests (Popa et al., 2010), whereas WAO is situated along the coast with less surrounding vegetation. Additionally, α_B at BIK is lower than at WAO due to a lower influence of crops and grasses at BIK, increasing the overestimation of α_B and increasing the bias at BIK.

We find that our APO-based fossil fuel CO_2 flux estimates are biased when using wrong values for α_B. The extent of this bias depends on the footprint that forms the atmospheric signal. To illustrate this, we selected three example days for WAO and BIK based on the atmospheric difference between the atmospheric fossil fuel CO_2 signal calculated using a constant value for α_B of 1.1 ($ff_{CO_2}[APO_{(\alpha_B = 1.1)}]$) and the true fossil fuel CO_2 signal (ff_{CO_2}[true]) (Figure A3 in the appendix). The difference in fossil fuel CO_2 mole fraction is not directly proportional to the bias in surface CO_2 flux estimations (Figure 8), but also includes the footprint of the observation (see Equation 9). When the atmospheric fossil fuel CO_2 signal is formed by a footprint covering a region with relatively low fossil fuel emissions (Figure A4b and A4e in the appendix) and strong biosphere influence (Figure A3 in the appendix), the relative difference between ff_{CO_2}[true] and $ff_{CO_2}[APO_{(\alpha_B = 1.1)}]$ increases. This leads to a corresponding increase in the estimated surface flux (Figures 8b and 8e). As a result, an overestimation of $ff_{CO_2}[APO_{(\alpha_B = 1.1)}]$ of 1.6 ppm at WAO could lead to an increase of 37% in fossil fuel surface fluxes, and an overestimation of 11.8 ppm at BIK could result in an overestimation of 197 TgC/yr inside the footprint. Conversely, when the footprint is dominated by regions

https://doi.org/10.5194/egusphere-2026-4491
Preprint. Discussion started: 24 August 2026

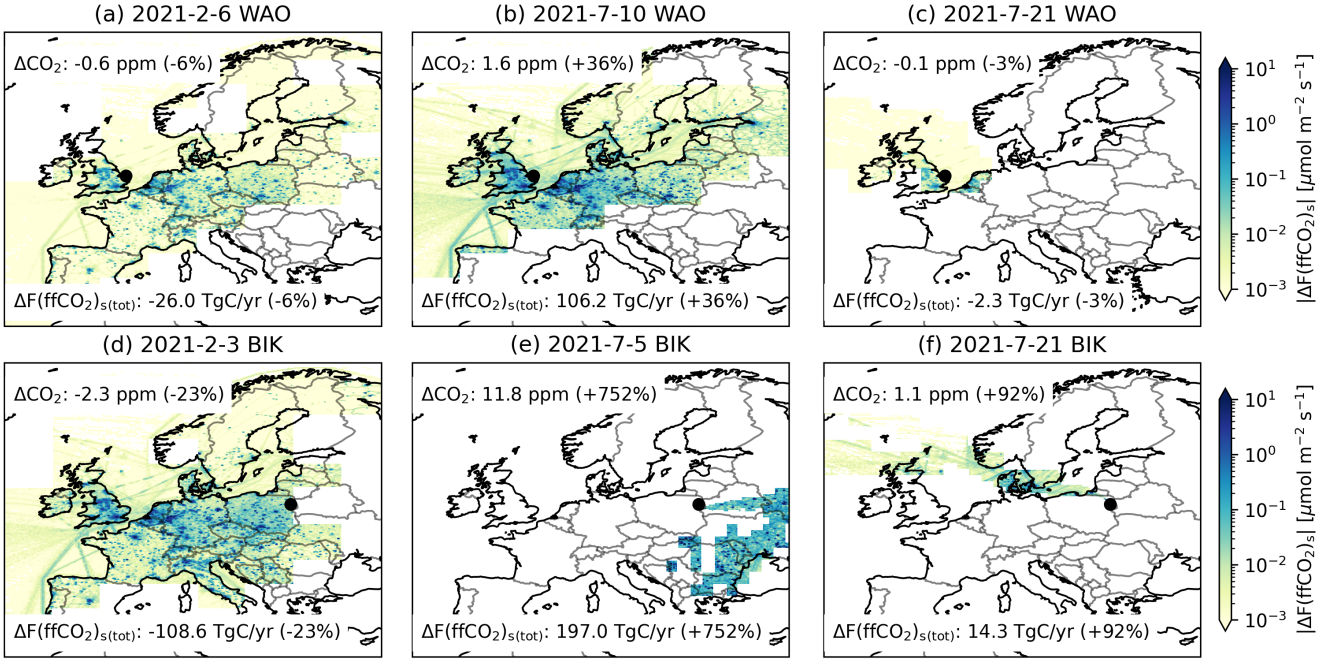

Figure 8. Difference between the fossil fuel CO_2 surface fluxes of the true STILT input fluxes from GridFED ($F(ff_{CO_2})_s$[true]) and the surface fluxes based on the APO fossil fuel signal with an α_B of 1.1 ($F(ff_{CO_2})_s[APO_{(\alpha_B = 1.1)}]$), calculated with Eq. 11, for footprints of three example days at Weybourne (WAO, a-c) and three days at Białystok (BIK, d-f) in units of μmol m^{-2} s^{-1}. Text labels: ΔCO_2 is the difference between the atmospheric signals of $ff_{CO_2}[APO_{(\alpha_B = 1.1)}]$ and ff_{CO_2}[true] (Figure A3), $\Delta F(ffCO_2)_{s(tot)}$ is the integrated difference between the surface fluxes of $F(ff_{CO_2})_s[APO_{(\alpha_B = 1.1)}]$ and $F(ff_{CO_2})_s$[true] inside the footprint, scaled to an annual flux.

with high fossil fuel emissions (Figure A4a and A4d in the appendix), the relative difference in CO_2 mole fraction is smaller, reducing the bias in surface flux estimation (Figures 8a and 8d). Overall, when using an assumed value for α_B of 1.1 instead of the 'true' α_B from SiB4 simulations, fossil fuel surface fluxes at BIK experience a greater bias compared to WAO. This is due to a stronger biospheric influence and lower fossil fuel contribution within the footprint at BIK.

4 Discussion

We presented first insights into global biospheric O_2 fluxes and the variability of ER_{net} by incorporating distinct exchange ratios for assimilation and respiration processes into the SiB4 model. This implementation revealed that ER_{net} shows a pronounced temporal variability at both global and European scales, alongside distinct spatial variations during the summer months in Europe. The modeled temporal and spatial variability of ER_{net} could significantly impact the application of the O_2 partitioning method for estimating fossil fuel CO_2 signals using APO (depending of the implementation), especially in situations where

https://doi.org/10.5194/egusphere-2026-4491
Preprint. Discussion started: 24 August 2026

the biosphere signals are large. In this section, we discuss the implementation of O_2 into the SiB4 model, explore how this approach can be validated and improved, and clarify the implications of our findings for other O_2 partitioning methods.

4.1 Evaluation of the O_2 implementation

The O_2 implementation into the SiB4 model should be validated with observations before using the resulting ER values. Several measurement locations are available that could provide above-vegetation O_2 flux observations to support validation of the SiB4 model. Since no direct O_2 flux measurement techniques are available, two measurement heights are needed to infer the O_2 fluxes. Locations that measure O_2 at two heights (or measured in the past) include: the WLEF-TV tower in Park Falls, Wisconsin, USA (Stephens et al., 2007), the Takayama tower (TKY) in Japan (Ishidoya et al., 2013), the Zotino Tall Tower Observatory (ZOTTO) in Russia (Kozlova and Manning, 2009), the Białystok tower in Poland (Popa et al., 2010), the Ochsenkopf tower in Germany (Thompson et al., 2009), the Reinshof site in Germany (Knohl et al., 2020), the Hyytiälä tower in Finland (Faassen et al., 2023), and since recently the Cabauw tower in the Netherlands (Luijkx and de Beijl, 2025). Data from these measurement towers could be used to evaluate the seasonal and annual patterns of ER_{net} by calculating O_2 and CO_2 surface fluxes based on their vertical gradients (Ishidoya et al., 2015; Faassen et al., 2023). Similar to the approach described in Faassen et al. (2023), ER_a and ER_r could be estimated at these locations using the GPP and TER fluxes. However, some of the above mentioned stations are discontinued and their records miss the necessary meteorological data to directly infer the surface fluxes. Additionally, inferring O_2 surface fluxes from a vertical gradient has been shown to be challenging (Ishidoya et al., 2015; Faassen et al., 2023), making validation of the ER_{net} values based on observational data difficult.

Besides the O_2 measurement stations mentioned above, further stations exist where O_2 mole fractions are measured at a single height above the surface. These single-height measurements of atmospheric O_2 and CO_2 mole fractions cannot be used to evaluate O_2 and CO_2 fluxes and their ER_{net} from the SiB4 model. The temporal variability of these compounds can only be used to derive ER_{atmos} ($\Delta O_{2(t)}/\Delta CO_{2(t)}$) (Faassen et al., 2023). While ER_{atmos} and single-height measurements may be useful for e.g. evaluating the combined atmospheric signal produced by atmospheric transport models such as STILT, as illustrated by the time series in Figure 7, they are not directly representative of surface exchange processes. As demonstrated in Faassen et al. (2024) and Faassen et al. (2025), ER_{atmos} cannot be linked to surface fluxes directly, because it is also influenced by atmospheric processes. The resulting ER_{atmos} therefore cannot be linked to a specific process anymore. For this reason, ER_{atmos} cannot be used to validate the temporal variability of ER_{net} values modeled with SiB4. To infer ER_{net} at measurement stations with O_2 measurements at only a single measurement height, these stations should therefore add at least one additional measurement height above the canopy.

A few additional improvements to the model implementation could help evaluate its accuracy without solely relying on observational data. The individual ER values in Table 1 are currently difficult to validate because of measurement challenges. However, theoretical approaches have demonstrated that O_2 uptake by the soil can be modeled independently from the CO_2

https://doi.org/10.5194/egusphere-2026-4491
Preprint. Discussion started: 24 August 2026

flux, using a vertical diffusion approach (Cook and Knight, 2003; Cook et al., 2013). Incorporating this modeling approach as a separate total O_2 soil flux into the SiB4 model and comparing it with the resulting O_2 soil fluxes derived from the current ER implementation could provide valuable insights. Discrepancies between these methods would serve as an initial indication of the model's capacity to reproduce O_2 soil fluxes accurately. Another method to support validation is the inclusion of stable isotope measurements, specifically $\delta^{13}C$ in CO_2. Studies have shown that $\delta^{13}C$ measurements can be used to explain ER measurements (Bowling et al., 2008; Hilman et al., 2019). For instance, when analyzing whether different substrates are being burned or formed, both $\delta^{13}C$ and ER_r or ER_a should have a similar change over time. By using the SiB4 implementation of $\delta^{13}C$ alongside O_2 (A. Kaushik, personal communication; Van der Velde et al., 2014), we could assess if ER and $\delta^{13}C$ behave similarly.

4.2 Additional measurements

Due to the highly challenging precision levels required to detect small differences in ER values, measurements are currently very limited. Therefore, more local biospheric measurements are essential to enhance our understanding of O_2 biosphere fluxes and to support our implementation of O_2 into the SiB4 model. This includes further development of additional measurement methodologies and techniques to reach the required levels of precision. Our findings highlight the priorities for such measurements. Existing measurement locations that have measured long-term atmospheric O_2 and CO_2 time series above the biosphere are limited, and are mainly located in temperate forest regions (as discussed above). Furthermore, our understanding of the different ER_a and ER_r signals from the biosphere remains limited due to measurement challenges. While it is impractical to measure every ER signal in detail for all plant functional types, our study offers valuable insights into prioritizing measurement efforts. Specifically, we have identified regions and ER signals that exert the most significant influence on the ER_{net} signal, guiding future research towards areas with the highest potential impact.

We found that especially more measurements are needed for crops. Figure 6 demonstrates that the spatial variation of the crop PFTs significantly contributes to the spatial pattern of ER_{net} during the summer, specifically the grass and general crop PFTs are of importance (Figure A5a in the appendix). This pattern arises from the assumption that ER_a and $ER_{r(auto)}$ values of crops are equal to their OR values (Gallagher et al., 2014). This assumption could be validated by measuring O_2 and CO_2 fluxes over a complete growing season of a specific crop and comparing it with the observed OR at the end of the growing season (by elemental composition analysis of the organic material that has formed over that time period). If the net O_2 and CO_2 exchange aligns with the measured OR, then the assumption holds. Moreover, the specific value of the OR should also be validated. We tested in a sensitivity experiment that when the ER_a and $ER_{r(auto)}$ of either grass or the general crops would increase by 0.1, locally the ER_{net} could increase by 0.2 (Figure A6a and Figure A6b in the appendix).

Additionally, the tropical region requires more attention. Figure A2 in the appendix reveals no clear seasonal pattern for this region, with extreme ER_{net} values fluctuating below 0.7 and above 1.3 throughout the year. The tropical ER_{net} signals might be influenced by factors other than the typical mid-latitude seasonal change (summer vs winter), such as El Niño events (van

https://doi.org/10.5194/egusphere-2026-4491
Preprint. Discussion started: 24 August 2026

Schaik et al., 2018), dry and wet periods (Restrepo-Coupe et al., 2013; Baldocchi et al., 2018) or biotic changes in leaf phenology (Wu et al., 2017). Given the high gross fluxes in the tropics compared to other regions (Luyssaert et al., 2007; Baldocchi et al., 2018), their impact on biospheric ER_{net} values is potentially substantial. However, the absence of long-term O_2 above canopy gradient measurements from tropical regions, and lack of CO_2 measurements as well, makes detailed analysis and model validation difficult.

When measuring ER values of an ecosystem, it is crucial to ensure that the correct measurements are taken by focusing on both the net exchange at the canopy level and the individual ER_a and ER_r values for leaves, stems and roots and heterotrophic respiration. To accurately calculate ER_{net} signals for the biosphere, either direct O_2 flux measurement methods need to be developed, or otherwise mole fraction measurements at a minimum of two heights and additional meteorological variables are needed, including the sensible heat flux to infer the net O_2 and CO_2 surface fluxes (Faassen et al., 2023). Relying on a single-height measurements could lead to incorrect ER_{net} values (Faassen et al., 2024). Additionally, individual ER_a and ER_r signals must also be measured to fully understand the ER_{net} signal. Particular emphasis should be placed on measuring ER signals from leaves, stems and roots, as there is currently no consensus on the processes shaping these signals. For the SiB4 implementation, we based stem and root ER signals on theoretical assumptions, with a constant value of 1.0. However, if the ER values of stems and roots deviate from this assumption, as some measurements suggest (Shane et al., 2004; Bathellier et al., 2009; Hilman et al., 2019, 2022), differences in spatial patterns would arise. This could especially be important for leaves and fine roots, as they are the main contributors to the autotrophic respiration in SiB4 (Figure A5b in the appendix). Our sensitivity tests show that increasing the $ER_{r(auto)}$ to 1.1 for either leaves or fine roots, can locally decrease the ER_{net} by 0.25 (Figure A6c and Figure A6d in the appendix).

4.3 Consequences for O_2 partitioning methods

Our first calculations of biosphere O_2 and CO_2 fluxes derived with SiB4 cannot yet replace the use of a constant value used for α_B in global, decadal scale O_2-based land and ocean carbon sink partitioning methods. When we average the global O_2 and CO_2 fluxes over 2021 (Figure 3), we found that the resulting ER_{net} value was approximately 0.42, which is unrealistic for the long-term mean biosphere exchange, and a result of averaging asymptotic values for periods when NEE is close to zero. Global-scale O_2 partitioning methods, which operate on decadal timescales, assume that ER_a and ER_r are equal and that OR values provide a reasonable proxy for the global ER_{net} or α_B value, resulting in the choice to use a constant value in the range of 1.05-1.1 for α_B based on OR measurements (Keeling, 1988; Severinghaus, 1995; Stephens et al., 1998; Worrall et al., 2013). With our current O_2 implementation in the SiB4 model, we cannot assess whether ER_a approaches ER_r over longer timescales, as we did not implement dynamical changes over time in the individual ER signals that show evolution over time associated with development of the vegetation and soil pools. Our global ER_{net} value therefore remains consistently lower than ER_a, yielding α_B values below 1.0, even over decadal timescales. It is likely that these low ER_{net} values do not reflect reality on decadal time scales, as it is often hypothesized that ER_{net} should converge to the OR when considering the complete

https://doi.org/10.5194/egusphere-2026-4491
Preprint. Discussion started: 24 August 2026

development of a vegetation type (Seibt et al., 2004; Randerson et al., 2006; Gallagher et al., 2014).

However, Randerson et al. (2006) hypothesized that small differences between ER_r and ER_a could arise on global decadal scale due to increased levels of human disturbance. As a result, ER_a and ER_r would no longer be in equilibrium. Consequently, the individual gross GPP and TER fluxes and their respective ER signals have to be taken into account in global scale O_2 partitioning methods, rather than the aggregated NEE flux and its ER_{net} or OR. Randerson et al. (2006) showed that a small difference of 0.0017 between ER_a and ER_r could already result in a shift of 0.1 PgC yr^{-1} from the global ocean to the land sink.

To re-evaluate the accuracy of the value used for α_B (1.05-1.1) on decadal timescales globally, temporal changes in ER_a and ER_r values associated with the current growth stage of the vegetation and carbon pools would need to be incorporated into the SiB4 model (as also proposed by Randerson et al. (2006)). This would require a more detailed implementation of vegetation development and of the corresponding molecular carbon (C), hydrogen (H), nitrogen (N) and oxygen (O) composition of the pools. Currently, the spin-up of the model ensures that the forest plant functional types and soil pools are in a steady state and further increases of the pools occur only due to environmental changes such as increases in temperature or atmospheric CO_2 mole fraction (Haynes et al., 2019). For grass and crop types, a complete growing cycle and different penological stages are already included (Haynes et al., 2019). If the complete development from seedling to fully grown vegetation were implemented for all vegetation types and if PFT's can be dynamically generated, such as is done in Dynamic Global Vegetation Models (DGVMs) (Sitch et al., 2024), ER values could vary between different stages of the development of the vegetation. Another method would be to model the molecular composition (C:H:N:O) of the carbon pools over time, which is now only done for carbon in the SiB4 model. This would make it possible to link the ER's of the fluxes directly to the OR. Both implementations would allow for a more accurate representation of temporal changes in ER_a and ER_r, caused by an ecosystem with changing carbon pool compositions. This could lead to a more reliable estimate of a single global ER_{net} value and provide insight into the appropriate value for α_B on different temporal and spatial scales.

For O_2 partitioning methods applied to smaller timescales or regional estimates of carbon budgets, the variability of ER_{net} (or α_B) could impact the results, depending on the method used and which location is analyzed. This variability is driven by the ratio between GPP and TER, and the values for ER_a and ER_r, and we recommend this variability to be considered. At the Weybourne site, the impact of incorporating a variable ER_{net} was less pronounced compared to Białystok, since there is less local vegetation activity. Other locations might experience a greater impact from a variable ER_{net} due to higher biosphere contributions or lower crop influence. It is important to note that our analysis does not account for variability in non-local biospheric signals originating from outside Europe (Figure 2) which could add further uncertainty. In the observational based method by Pickers et al. (2022), no distinction is made between the values used for α_B for the background signal and the perturbations from the background signal. For the case of WAO that works well (see Figure 7i). However, at stations with a high biosphere influence, like BIK, the impact of using an incorrect α_B value for the perturbations from the background would be larger. Therefore, using APO to derive fossil fuel CO_2 signals is expected to give better results at locations with relatively

https://doi.org/10.5194/egusphere-2026-4491
Preprint. Discussion started: 24 August 2026

low influence from the biosphere to reduce the potential bias resulting from a variable α_B.

5 Conclusions

By incorporating O_2 into the simple biosphere model (SiB4), we demonstrated that the net O_2 to CO_2 exchange ratio (ER_{net}) of the biosphere on regional to local spatial scales cannot be assumed to be a constant value, but that ER_{net} is characterized by temporal and spatial variability. The temporal variability arises from differences in the ratio between gross primary productivity (GPP) and total ecosystem respiration (TER), leading to a distinct seasonal pattern. We find large differences between regions, corresponding to differences in plant functional types between e.g the tropics and the boreal regions. Although our O_2 implementation in SiB4 was based on theoretical assumptions and limited available measurements of the oxidative ratios, we show that it is likely that ER_{net} is not constant, but varies temporally and spatially, because the variability depends on temporal changes of the ratio between GPP and TER and spatial differences in plant function types. However, to determine exact values of ER_{net}, the model needs to be further validated.

Certain atmospheric potential oxygen (APO) based methods to derive fossil fuel CO_2 signals can lead to overestimated in summertime (or underestimation during wintertime) atmospheric fossil fuel CO_2 signals and emissions when variability in ER_{net} is not accounted for. The overestimation is highest when the contribution from the biosphere to the total CO_2 signal is high and when the true ER_{net} value deviates further from the assumed constant value (typically 1.05-1.1). Additionally, the relative bias in the fossil fuel emissions increases when the footprint of the signal includes smaller fossil fuel fluxes. For future applications of O_2 partitioning methods, our O_2 implementation in SiB4 could provide a first estimate for variable ER_{net} values.

Due to the lack of temporal changes in the ER_a and ER_r values in our model implementation, associated with carbon pool growth, it is not possible yet to use the resulting global average ER_{net} value from SiB4 in global O_2-based land versus ocean carbon sink partitioning methods. On the decadal time scales for which these global partitioning methods are applied, it is assumed that ER_a and ER_r have the same value resulting in a constant ER_{net}. We could not validate this assumption with the current set-up of the model because the implemented ER_a and ER_r values stay constant over time. Consequently, we cannot address the potential temporal variability of the constant value of 1.05-1.1 used on the global spatial and decadal time scales. More detailed implementation in SiB4 is needed to evaluate the value of α_B, and this improvement should be rooted in expanded high-precision multi-level observations of O_2 and CO_2.

https://doi.org/10.5194/egusphere-2026-4491
Preprint. Discussion started: 24 August 2026

Appendix A: Figures

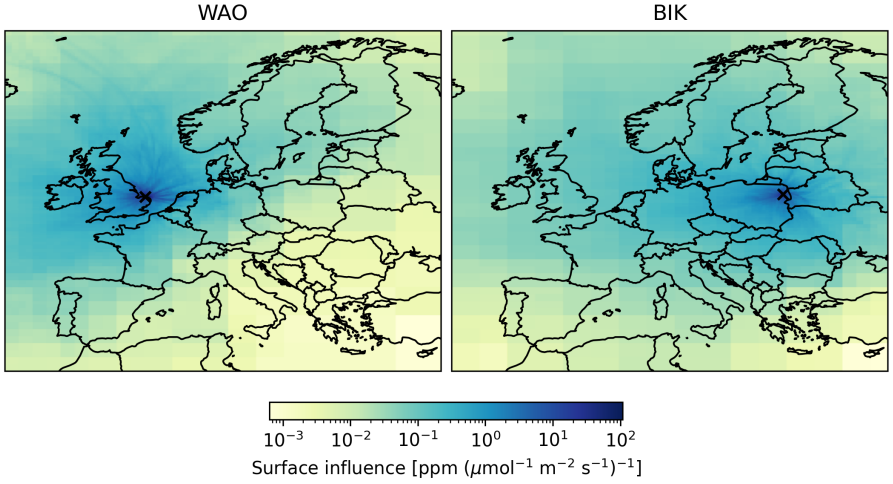

Figure A1. Sum of the footprint influence during 2021, for the stations: Weybourne (WAO) in the UK and Białystok (BIK) in Poland, calculated by the STILT model.

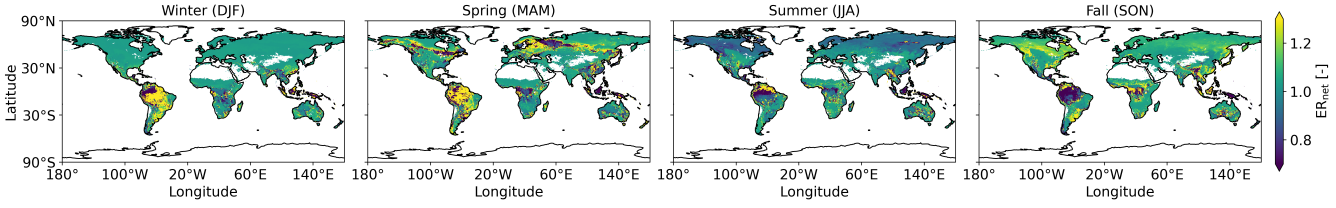

Figure A2. Averaged values of the SiB4 model results during the seasons: winter (December - February, DJF), spring (March - May, MAM), summer (June - August, JJA) and fall (September - November, SON) for the net exchange ratio (ER_{net}).

https://doi.org/10.5194/egusphere-2026-4491
Preprint. Discussion started: 24 August 2026

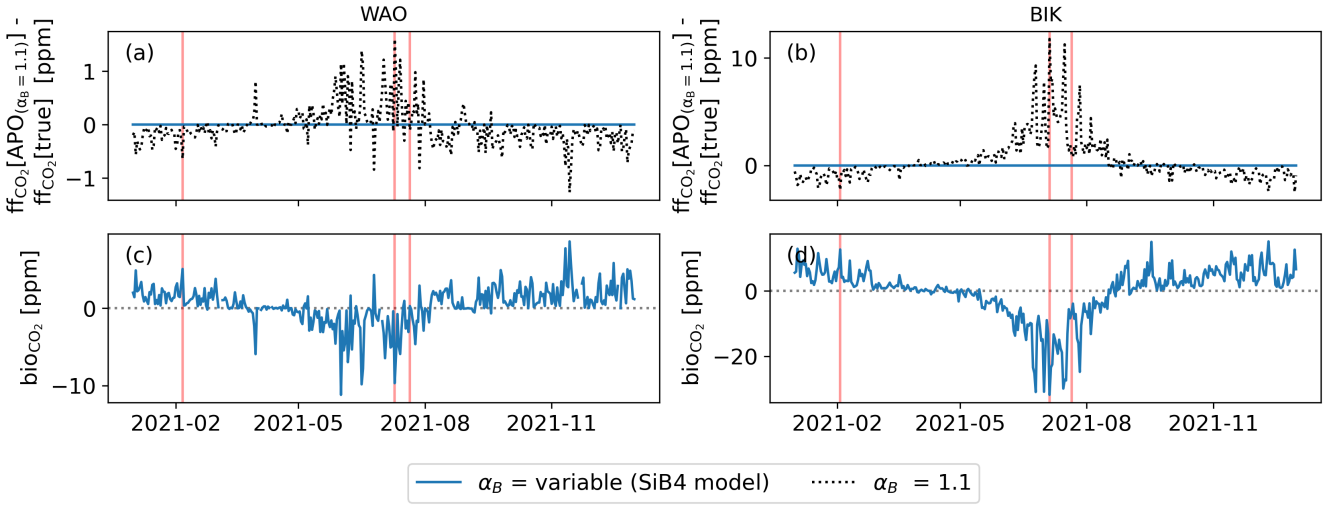

Figure A3. Timeseries of the transported surface fluxes by STILT and the resulting difference between the fossil fuel signal estimated with atmospheric potential oxygen ($ff_{CO_2}[APO_{(\alpha_B = 1.1)}]$) and the true fossil fuel signal ($ff_{CO_2}[true]$) (a,b), together with the biosphere signals (c,d) for the stations Weybourne (WAO, a, c) and Białystok (BIK, b, d)

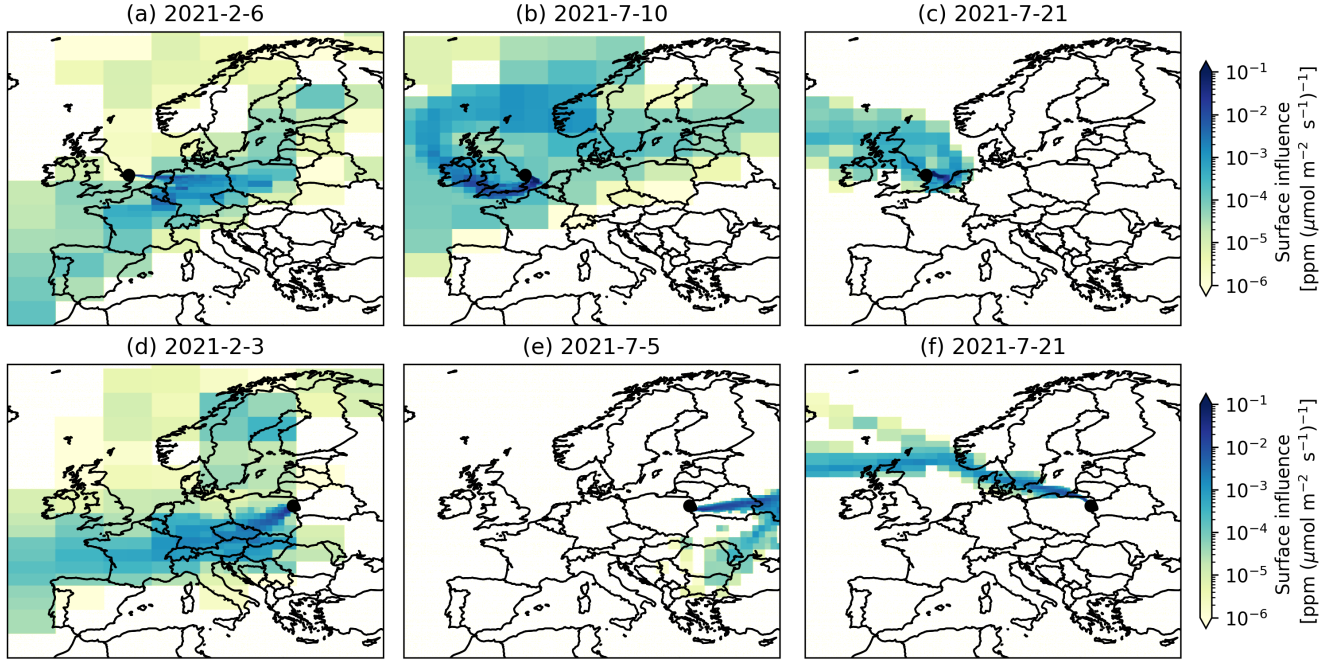

Figure A4. The footprint influence for three individual days at Weybourne (a-c) and Białystok (d-f).

https://doi.org/10.5194/egusphere-2026-4491
Preprint. Discussion started: 24 August 2026

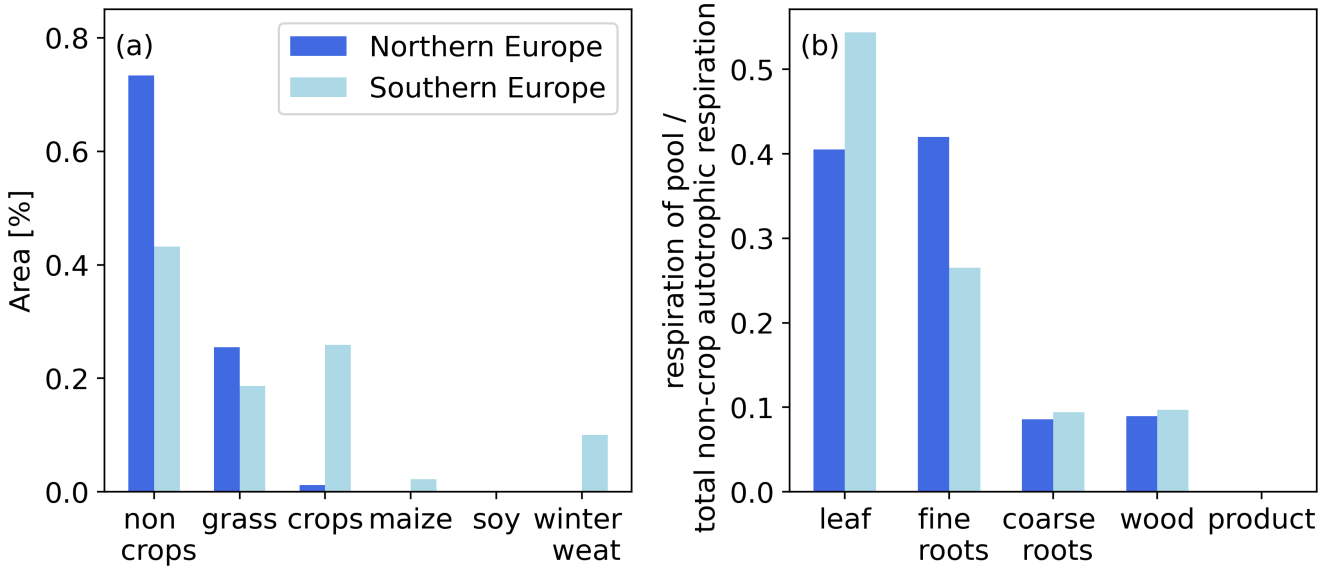

Figure A5. Contribution of the different plant functional types (PFT) to the total area (a) and the contribution of non-crop PFT carbon pools to the total autotrophic respiration formed by non-crop PFTs (b) for northern (between 60°N and 80°N) and southern (between 30°N and 60°N) Europe.

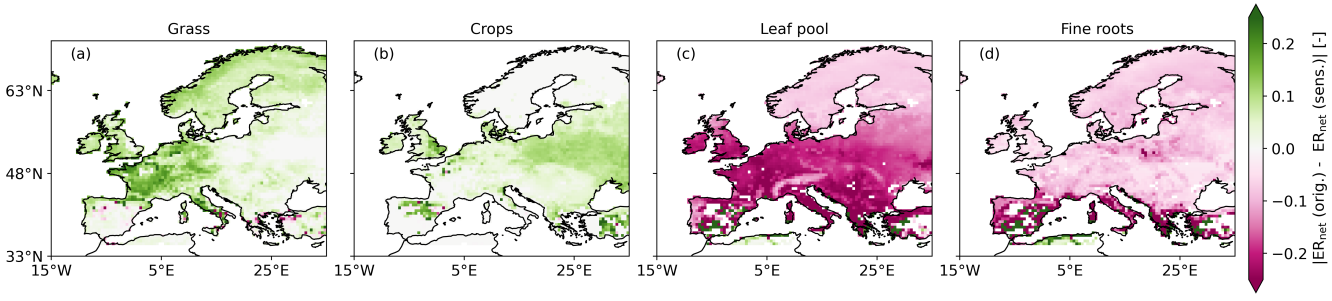

Figure A6. Difference between the exchange ratio as used in the main text (ER_{net} (orig.)) based on the implementation of Table 1 and the exchange ratio as used in the sensitivity tests (ER_{net} (sens.)) where the ER was increased by 0.1 for grass (a), crops (b), leaf pool (c) and fine roots pool (d). For grass and crops, both the ER_a and $ER_{r(auto)}$ were adjusted, and for the leaf and fine roots pool only $ER_{r(auto)}$ was adjusted.

https://doi.org/10.5194/egusphere-2026-4491
Preprint. Discussion started: 24 August 2026

Code availability. The model code of SiB4 is available on https://gitlab.com/kdhaynes/sib4v2_corral, of TM5 on https://sourceforge.net/projects/tm5/ and of STILT on https://stilt-model.org/.

Author contributions. KF developed the O_2 implementation for SiB4 and performed the analysis. AvdW preformed the STILT model simulations. JH performed the TM5 model simulations. AK and BH contributed to the SiB4 implementation. KF, ITL, and WP designed the study and interpreted and discussed the results. KF wrote the manuscript with input from all co-authors.

Competing interests. There are no competing interests.

Acknowledgements. The authors would like to thank Anne-Wil van den Berg (Meteorology and Air Quality (MAQ), Wageningen University and Research (WUR), Wageningen, the Netherlands), Marnix van de Sande (MAQ-WUR) and Remco de Kok (previously at MAQ-WUR) for their help with setting up the SiB4 model. Furthermore, we would like to thank Lucas Hulsman (MAQ-WUR) for his input on the O_2 implementation in the SiB4 model. We have used ChatGPT as a language editor to improve the readability of certain parts of the manuscript. This work was supported by funding from the Netherlands Organisation for Scientific Research (grant no. VI.Vidi.213.143), as well as by the Horizon Europe CORSO project (no. 101082194). We thank SURF Cooperative for the support in using the National Supercomputer Snellius for the model simulations (project number NWO-2023.003).

https://doi.org/10.5194/egusphere-2026-4491
Preprint. Discussion started: 24 August 2026

References

Adcock, K. E., Pickers, P. A., Manning, A. C., Forster, G. L., Fleming, L. S., Barningham, T., Wilson, P. A., Kozlova, E. A., Hewitt, M., Etchells, A. J., et al.: 12 years of continuous atmospheric O 2, CO 2 and APO data from Weybourne Atmospheric Observatory in the United Kingdom, Earth System Science Data, 15, 5183–5206, 2023.

Angert, A., Yakir, D., Rodeghiero, M., Preisler, Y., Davidson, E. A., and Weiner, T.: Using O_2 to study the relationships between soil CO_2 efflux and soil respiration, Biogeosciences, 12, 2089–2099, https://doi.org/10.5194/bg-12-2089-2015, 2015.

Aubrey, D. P. and Teskey, R. O.: Root-derived CO2 efflux via xylem stream rivals soil CO2 efflux, New Phytologist, 184, 35–40, 2009.

Baldocchi, D., Chu, H., and Reichstein, M.: Inter-annual variability of net and gross ecosystem carbon fluxes: A review, Agricultural and Forest Meteorology, 249, 520–533, 2018.

Bathellier, C., Tcherkez, G., Bligny, R., Gout, E., Cornic, G., and Ghashghaie, J.: Metabolic origin of the δ13C of respired CO2 in roots of Phaseolus vulgaris, New Phytologist, 181, 387–399, 2009.

Battle, M. O., William Munger, J., Conley, M., Sofen, E., Perry, R., Hart, R., Davis, Z., Scheckman, J., Woogerd, J., Graeter, K., Seekins, S., David, S., and Carpenter, J.: Atmospheric measurements of the terrestrial O_2 : CO_2 exchange ratio of a midlatitude forest, Atmospheric Chemistry and Physics, 19, 8687–8701, https://doi.org/10.5194/acp-19-8687-2019, 2019.

Bloom, A. J.: Photorespiration and nitrate assimilation: a major intersection between plant carbon and nitrogen, Photosynthesis research, 123, 117–128, 2015.

Bowling, D. R., Pataki, D. E., and Randerson, J. T.: Carbon isotopes in terrestrial ecosystem pools and CO2 fluxes, New Phytologist, 178, 24–40, 2008.

Bruhn, D., Fan, Y., Griffin, K. L., Cowan-Turner, D., Scafaro, A. P., Møller, I. M., and Atkin, O. K.: Importance of the leaf respiratory quotient, Physiologia Plantarum, 177, e70 235, 2025.

Clay, G. D. and Worrall, F.: Oxidative ratio (OR) of Southern African soils and vegetation: Updating the global OR estimate, Catena, 126, 126–133, 2015.

Cook, F. and Knight, J.: Oxygen transport to plant roots: modeling for physical understanding of soil aeration, Soil Science Society of America Journal, 67, 20–31, 2003.

Cook, F., Knight, J., and Kelliher, F.: Modelling oxygen transport in soil with plant root and microbial oxygen consumption: depth of oxygen penetration, Soil Research, 51, 539–553, 2013.

Cousins, A. and Bloom, A.: Oxygen consumption during leaf nitrate assimilation in a C3 and C4 plant: the role of mitochondrial respiration, Plant, Cell & Environment, 27, 1537–1545, 2004.

De Vries, F. P., Brunsting, A., and Van Laar, H.: Products, requirements and efficiency of biosynthesis a quantitative approach, Journal of theoretical Biology, 45, 339–377, 1974.

Ding, L., Huang, J., Li, C., Han, D., Liu, X., Li, H., Bai, Y., and Huang, J.: Variations in terrestrial oxygen sources under climate change, Science China Earth Sciences, 65, 1810–1823, 2022.

Faassen, K. A., Nguyen, L. N., Broekema, E. R., Kers, B. A., Mammarella, I., Vesala, T., Pickers, P. A., Manning, A. C., Vilà-Guerau de Arellano, J., Meijer, H. A., et al.: Diurnal variability of atmospheric O_2, CO_2, and their exchange ratio above a boreal forest in southern Finland, Atmospheric Chemistry and Physics, 23, 851–876, 2023.

https://doi.org/10.5194/egusphere-2026-4491
Preprint. Discussion started: 24 August 2026

Faassen, K. A., Vilà-Guerau de Arellano, J., González-Armas, R., Heusinkveld, B. G., Mammarella, I., Peters, W., and Luijkx, I. T.: Separating above-canopy CO 2 and O 2 measurements into their atmospheric and biospheric signatures, Biogeosciences, 21, 3015–3039, 2024.

Faassen, K. A., González-Armas, R., Koren, G., Adnew, G. A., van Asperen, H., de Boer, H., Botía, S., de Feiter, V. S., Hartogensis, O., Heusinkveld, B. G., et al.: Tracing Diurnal Variations of Atmospheric CO2, O2, and δ 13 δˆ13 CO2 Over a Tropical and a Temperate Forest, Geophysical Research Letters, 52, e2025GL118 016, 2025.

Fischer, S., Hanf, S., Frosch, T., Gleixner, G., Popp, J., Trumbore, S., and Hartmann, H.: Pinus sylvestris switches respiration substrates under shading but not during drought, New Phytologist, 207, 542–550, 2015.

Friedlingstein, P., O'Sullivan, M., Jones, M. W., Andrew, R. M., Bakker, D. C. E., Hauck, J., Landschützer, P., Le Quéré, C., Li, H., Luijkx, I. T., Peters, G. P., Peters, W., Pongratz, J., Schwingshackl, C., Sitch, S., Canadell, J. G., Ciais, P., Aas, K., Alin, S. R., Anthoni, P., Barbero, L., Bates, N. R., Bellouin, N., Benoit-Cattin, A., Berghoff, C. F., Bernardello, R., Bopp, L., Brasika, I. B. M., Chamberlain, M. A., Chandra, N., Chevallier, F., Chini, L. P., Collier, N. O., Colligan, T. H., Cronin, M., Djeutchouang, L., Dou, X., Enright, M. P., Enyo, K., Erb, M., Evans, W., Feely, R. A., Feng, L., Ford, D. J., Foster, A., Fransner, F., Gasser, T., Gehlen, M., Gkritzalis, T., Goncalves De Souza, J., Grassi, G., Gregor, L., Gruber, N., Guenet, B., Gürses, O., Harrington, K., Harris, I., Heinke, J., Hurtt, G. C., Iida, Y., Ilyina, T., Ito, A., Jacobson, A. R., Jain, A. K., Jarníková, T., Jersild, A., Jiang, F., Jones, S. D., Kato, E., Keeling, R. F., Klein Goldewijk, K., Knauer, J., Kong, Y., Korsbakken, J. I., Koven, C., Kunimitsu, T., Lan, X., Liu, J., Liu, Z., Liu, Z., Lo Monaco, C., Ma, L., Marland, G., McGuire, P. C., McKinley, G. A., Melton, J., Monacci, N., Monier, E., Morgan, E. J., Munro, D. R., Müller, J. D., Nakaoka, S.-I., Nayagam, L. R., Niwa, Y., Nutzel, T., Olsen, A., Omar, A. M., Pan, N., Pandey, S., Pierrot, D., Qin, Z., Regnier, P. A. G., Rehder, G., Resplandy, L., Roobaert, A., Rosan, T. M., Rödenbeck, C., Schwinger, J., Skjelvan, I., Smallman, T. L., Spada, V., Sreeush, M. G., Sun, Q., Sutton, A. J., Sweeney, C., Swingedouw, D., Séférian, R., Takao, S., Tatebe, H., Tian, H., Tian, X., Tilbrook, B., Tsujino, H., Tubiello, F., van Ooijen, E., van der Werf, G., van de Velde, S. J., Walker, A., Wanninkhof, R., Yang, X., Yuan, W., Yue, X., and Zeng, J.: Global Carbon Budget 2025, Earth System Science Data Discussions, 2025, 1–139, https://doi.org/10.5194/essd-2025-659, 2025.

Gallagher, M., Masiello, C., Hockaday, W., Baldock, J., Snapp, S., and McSwiney, C.: Controls on the oxidative ratio of net primary production in agricultural ecosystems, Biogeochemistry, 121, 581–594, 2014.

Gauthier, P. P., Battle, M. O., Griffin, K. L., and Bender, M. L.: Measurement of gross photosynthesis, respiration in the light, and mesophyll conductance using H2 18O labeling, Plant Physiology, 177, 62–74, 2018.

Gerbig, C., Lin, J., Wofsy, S., Daube, B., Andrews, A., Stephens, B., Bakwin, P., and Grainger, C.: Toward constraining regional-scale fluxes of CO2 with atmospheric observations over a continent: 2. Analysis of COBRA data using a receptor-oriented framework, Journal of Geophysical Research: Atmospheres, 108, 2003.

Haynes, K., Baker, I., Denning, A., Stöckli, R., Schaefer, K., Lokupitiya, E., and Haynes, J.: Representing grasslands using dynamic prognostic phenology based on biological growth stages: 1. Implementation in the Simple Biosphere Model (SiB4), Journal of Advances in Modeling Earth Systems, 11, 4423–4439, 2019.

Helm, J., Salomón, R. L., Hilman, B., Muhr, J., Knohl, A., Steppe, K., Gibon, Y., Cassan, C., and Hartmann, H.: Differences between tree stem CO2 efflux and O2 influx rates cannot be explained by internal CO2 transport or storage in large beech trees, Plant, Cell & Environment, 46, 2680–2693, 2023.

Hersbach, H., Bell, B., Berrisford, P., Hirahara, S., Horányi, A., Muñoz-Sabater, J., Nicolas, J., Peubey, C., Radu, R., Schepers, D., et al.: The ERA5 global reanalysis, Quarterly Journal of the Royal Meteorological Society, 146, 1999–2049, 2020.

https://doi.org/10.5194/egusphere-2026-4491
Preprint. Discussion started: 24 August 2026

Hicks Pries, C., Angert, A., Castanha, C., Hilman, B., and Torn, M. S.: Using respiration quotients to track changing sources of soil respiration seasonally and with experimental warming, Biogeosciences, 17, 3045–3055, 2020.

Hilman, B., Muhr, J., Trumbore, S. E., Kunert, N., Carbone, M. S., Yuval, P., Wright, S. J., Moreno, G., Pérez-Priego, O., Migliavacca, M., et al.: Comparison of CO 2 and O 2 fluxes demonstrate retention of respired CO 2 in tree stems from a range of tree species, Biogeosciences, 16, 177–191, 2019.

Hilman, B., Muhr, J., Helm, J., Kuhlmann, I., Schulze, E.-D., and Trumbore, S.: The size and the age of the metabolically active carbon in tree roots, Plant, Cell & Environment, 44, 2522–2535, 2021.

Hilman, B., Weiner, T., Haran, T., Masiello, C. A., Gao, X., and Angert, A.: The apparent respiratory quotient of soils and tree stems and the processes that control it, Journal of Geophysical Research: Biogeosciences, 127, e2021JG006 676, 2022.

Hoch, G., Richter, A., and Körner, C.: Non-structural carbon compounds in temperate forest trees, Plant, cell & environment, 26, 1067–1081, 2003.

Huang, J., Huang, J., Liu, X., Li, C., Ding, L., and Yu, H.: The global oxygen budget and its future projection, Science Bulletin, 63, 1180–1186, 2018.

Ishidoya, S., Murayama, S., Takamura, C., Kondo, H., Saigusa, N., Goto, D., Morimoto, S., Aoki, N., Aoki, S., and Nakazawa, T.: O_2:CO_2 exchange ratios observed in a cool temperate deciduous forest ecosystem of central Japan , Tellus B: Chemical and Physical Meteorology, 65, 21 120, https://doi.org/10.3402/tellusb.v65i0.21120, 2013.

Ishidoya, S., Murayama, S., Kondo, H., Saigusa, N., Kishimoto-Mo, A. W., and Yamamoto, S.: Observation of O_2:CO_2 exchange ratio for net turbulent fluxes and its application to forest carbon cycles, Ecological Research, 30, 225–234, https://doi.org/10.1007/s11284-014-1241-3, 2015.

Jones, M. W., Andrew, R. M., Peters, G. P., Janssens-Maenhout, G., De-Gol, A. J., Ciais, P., Patra, P. K., Chevallier, F., and Le Quéré, C.: Gridded fossil CO2 emissions and related O2 combustion consistent with national inventories 1959–2018, Scientific Data, 8, 2, 2021.

Jürgensen, J., Muhr, J., and Knohl, A.: Variations of the Oxidative Ratio across Ecosystem Components and Seasons in a Managed Temperate Beech Forest (Leinefelde, Germany), Forests, 12, 1693, 2021.

Keeling, R.: Development of an Interferometric Oxygen Analyzer for Precise Measurement of the Atmospheric O_2 Mole Fraction., Ph.D. thesis, Harvard University, 1988.

Keeling, R. and Manning, A.: Studies of recent changes in atmospheric O2 content, in: Treatise on Geochemistry: Second Edition, pp. 385–404, 2014.

Keeling, R. F., Manning, A. C., McEvoy, E. M., and Shertz, S. R.: Methods for measuring changes in atmospheric O_2 concentration and their application in southern hemisphere air, Journal of Geophysical Research: Atmospheres, 103, 3381–3397, 1998.

Knohl, A., Muhr, J., Deventer, M. J., Blei, E., Braden-Behrens, J., Tunsch, E., Bonazza, M., Pickers, P. A., Nelson, D., Zahniser, M., et al.: Measuring oxygen fluxes in a European beech forest-results from the OXYFLUX project, in: EGU General Assembly Conference Abstracts, p. 18822, 2020.

Kooijmans, L. M., Cho, A., Ma, J., Kaushik, A., Haynes, K. D., Baker, I., Luijkx, I. T., Groenink, M., Peters, W., Miller, J. B., et al.: Evaluation of carbonyl sulfide biosphere exchange in the Simple Biosphere Model (SiB4), Biogeosciences, 18, 6547–6565, 2021.

Kozlova, E. A. and Manning, A. C.: Methodology and calibration for continuous measurements of biogeochemical trace gas and O_2 concentrations from a 300-m tall tower in central Siberia, Atmospheric Measurement Techniques, 2, 205–220, https://doi.org/10.5194/amt-2-205-2009, 2009.

https://doi.org/10.5194/egusphere-2026-4491
Preprint. Discussion started: 24 August 2026

Krol, M., Houweling, S., Bregman, B., Van den Broek, M., Segers, A., Van Velthoven, P., Peters, W., Dentener, F., and Bergamaschi, P.: The two-way nested global chemistry-transport zoom model TM5: algorithm and applications, Atmospheric Chemistry and Physics, 5, 417–432, 2005.

Lin, J., Gerbig, C., Wofsy, S., Andrews, A., Daube, B., Davis, K., and Grainger, C.: A near-field tool for simulating the upstream influence of atmospheric observations: The Stochastic Time-Inverted Lagrangian Transport (STILT) model, Journal of Geophysical Research: Atmospheres, 108, 2003.

Luijkx, I. and de Beijl, L.: Atmospheric GHG data product (O_2, O_2 stdev, CO_2, CO_2 stdev) from Cabauw (207.0 m), https://doi.org/10.18160/0MED-MG1W, 2025.

Luyssaert, S., Inglima, I., Jung, M., Richardson, A. D., Reichstein, M., Papale, D., Piao, S., Schulze, E.-D., Wingate, L., Matteucci, G., et al.: CO2 balance of boreal, temperate, and tropical forests derived from a global database, Global change biology, 13, 2509–2537, 2007.

Manning, A. and Keeling, R. F.: Global oceanic and land biotic carbon sinks from the Scripps atmospheric oxygen flask sampling network, Tellus B: Chemical and Physical Meteorology, 58, 95–116, 2006.

Masiello, C., Gallagher, M., Randerson, J., Deco, R., and Chadwick, O.: Evaluating two experimental approaches for measuring ecosystem carbon oxidation state and oxidative ratio, Journal of Geophysical Research: Biogeosciences, 113, 2008.

McDermitt, D. and Loomis, R.: Elemental composition of biomass and its relation to energy content, growth efficiency, and growth yield, Annals of Botany, 48, 275–290, 1981.

Miller, J. B. and Tans, P. P.: Calculating isotopic fractionation from atmospheric measurements at various scales, Tellus B: Chemical and Physical Meteorology, 55, 207–214, 2003.

Pickers, P. A., Manning, A. C., Le Quéré, C., Forster, G. L., Luijkx, I. T., Gerbig, C., Fleming, L. S., and Sturges, W. T.: Novel quantification of regional fossil fuel CO2 reductions during COVID-19 lockdowns using atmospheric oxygen measurements, Science advances, 8, eabl9250, 2022.

Plaxton, W. C. and Podestá, F. E.: The functional organization and control of plant respiration, Critical Reviews in Plant Sciences, 25, 159–198, 2006.

Popa, M. E., Gloor, M., Manning, A. C., Jordan, A., Schultz, U., Haensel, F., Seifert, T., and Heimann, M.: Measurements of greenhouse gases and related tracers at Bialystok tall tower station in Poland, Atmospheric Measurement Techniques, 3, 407–427, https://doi.org/10.5194/amt-3-407-2010, 2010.

Rachmilevitch, S., Lambers, H., and Huang, B.: Root respiratory characteristics associated with plant adaptation to high soil temperature for geothermal and turf-type Agrostis species, Journal of Experimental Botany, 57, 623–631, 2006.

Randerson, J. T., Masiello, C., Still, C., Rahn, T., Poorter, H., and Field, C.: Is carbon within the global terrestrial biosphere becoming more oxidized? Implications for trends in atmospheric O2, Global Change Biology, 12, 260–271, 2006.

Restrepo-Coupe, N., da Rocha, H. R., Hutyra, L. R., da Araujo, A. C., Borma, L. S., Christoffersen, B., Cabral, O. M., de Camargo, P. B., Cardoso, F. L., da Costa, A. C. L., et al.: What drives the seasonality of photosynthesis across the Amazon basin? A cross-site analysis of eddy flux tower measurements from the Brasil flux network, Agricultural and Forest Meteorology, 182, 128–144, 2013.

Roberts, C. D., Senan, R., Molteni, F., Boussetta, S., Mayer, M., and Keeley, S. P.: Climate model configurations of the ECMWF Integrated Forecasting System (ECMWF-IFS cycle 43r1) for HighResMIP, Geoscientific model development, 11, 3681–3712, 2018.

Rödenbeck, C., Adcock, K. E., Eritt, M., Gachkivskyi, M., Gerbig, C., Hammer, S., Jordan, A., Keeling, R. F., Levin, I., Maier, F., et al.: The suitability of atmospheric oxygen measurements to constrain western European fossil-fuel CO 2 emissions and their trends, Atmospheric Chemistry and Physics, 23, 15 767–15 782, 2023.

https://doi.org/10.5194/egusphere-2026-4491
Preprint. Discussion started: 24 August 2026

Saglio, P. H. and Pradet, A.: Soluble sugars, respiration, and energy charge during aging of excised maize root tips, Plant physiology, 66, 516–519, 1980.

Seibt, U., Brand, W. A., Heimann, M., Lloyd, J., Severinghaus, J. P., and Wingate, L.: Observations of O_2 : CO_2 exchange ratios during ecosystem gas exchange, Global Biogeochemical Cycles, 18, 1–18, https://doi.org/10.1029/2004GB002242, 2004.

Severinghaus, J. P.: Studies of the terrestrial O2 and carbon cycles in sand dune gases and in Biosphere 2, Tech. rep., Oak Ridge Associated Universities, Inc., TN (United States), 1995.

Shane, M. W., Cramer, M. D., Funayama-Noguchi, S., Cawthray, G. R., Millar, A. H., Day, D. A., and Lambers, H.: Developmental physiology of cluster-root carboxylate synthesis and exudation in harsh hakea. Expression of phospho enol pyruvate carboxylase and the alternative oxidase, Plant Physiology, 135, 549–560, 2004.

Sitch, S., O'sullivan, M., Robertson, E., Friedlingstein, P., Albergel, C., Anthoni, P., Arneth, A., Arora, V. K., Bastos, A., Bastrikov, V., et al.: Trends and drivers of terrestrial sources and sinks of carbon dioxide: An overview of the TRENDY project, Global Biogeochemical Cycles, 38, e2024GB008 102, 2024.

Smith, N. E., Kooijmans, L. M., Koren, G., Van Schaik, E., van Der Woude, A. M., Wanders, N., Ramonet, M., Xueref-Remy, I., Siebicke, L., Manca, G., et al.: Spring enhancement and summer reduction in carbon uptake during the 2018 drought in northwestern Europe, Philosophical Transactions of the Royal Society B, 375, 20190 509, 2020.

Steinbach, J., Gerbig, C., Rödenbeck, C., Karstens, U., Minejima, C., and Mukai, H.: The CO 2 release and Oxygen uptake from Fossil Fuel Emission Estimate (COFFEE) dataset: effects from varying oxidative ratios, Atmospheric Chemistry and Physics, 11, 6855–6870, 2011.

Stephens, B. B., Keeling, R. F., Heimann, M., Six, K. D., Murnane, R., and Caldeira, K.: Testing global ocean carbon cycle models using measurements of atmospheric O_2 and CO_2 concentration, Global Biogeochemical Cycles, 12, 213–230, https://doi.org/10.1029/97GB03500, 1998.

Stephens, B. B., Bakwin, P. S., Tans, P. P., Teclaw, R. M., and Baumann, D. D.: Application of a differential fuel-cell analyzer for measuring atmospheric oxygen variations, Journal of Atmospheric and Oceanic Technology, 24, 82–94, https://doi.org/10.1175/JTECH1959.1, 2007.

Suleau, M., Moureaux, C., Dufranne, D., Buysse, P., Bodson, B., Destain, J.-P., Heinesch, B., Debacq, A., and Aubinet, M.: Respiration of three Belgian crops: partitioning of total ecosystem respiration in its heterotrophic, above-and below-ground autotrophic components, Agricultural and Forest Meteorology, 151, 633–643, 2011.

Teskey, R. O., Saveyn, A., Steppe, K., and McGuire, M. A.: Origin, fate and significance of CO 2 in tree stems., New Phytologist, 177, 2008.

Thompson, R., Manning, A., Gloor, E., Schultz, U., Seifert, T., Hänsel, F., Jordan, A., and Heimann, M.: In-situ measurements of oxygen, carbon monoxide and greenhouse gases from Ochsenkopf tall tower in Germany, Atmospheric Measurement Techniques, 2, 573–591, 2009.

Van der Velde, I., Miller, J., Schaefer, K., Van Der Werf, G., Krol, M., and Peters, W.: Terrestrial cycling of 13 CO 2 by photosynthesis, respiration, and biomass burning in SiBCASA, Biogeosciences, 11, 6553–6571, 2014.

Van Der Woude, A. M., De Kok, R., Smith, N., Luijkx, I. T., Botía, S., Karstens, U., Kooijmans, L. M., Koren, G., Meijer, H. A., Steeneveld, G.-J., et al.: Near-real-time CO 2 fluxes from CarbonTracker Europe for high-resolution atmospheric modeling, Earth System Science Data, 15, 579–605, 2023a.

Van Der Woude, A. M., Peters, W., Joetzjer, E., Lafont, S., Koren, G., Ciais, P., Ramonet, M., Xu, Y., Bastos, A., Botía, S., et al.: Temperature extremes of 2022 reduced carbon uptake by forests in Europe, nature communications, 14, 6218, 2023b.

https://doi.org/10.5194/egusphere-2026-4491
Preprint. Discussion started: 24 August 2026

van Schaik, E., Killaars, L., Smith, N. E., Koren, G., Van Beek, L., Peters, W., and van der Laan-Luijkx, I. T.: Changes in surface hydrology, soil moisture and gross primary production in the Amazon during the 2015/2016 El Niño, Philosophical Transactions of the Royal Society B: Biological Sciences, 373, 20180 084, 2018.

Worrall, F., Clay, G. D., Masiello, C. A., and Mynheer, G.: Estimating the oxidative ratio of the global terrestrial biosphere carbon, Biogeochemistry, 115, 23–32, 2013.

Wu, J., Guan, K., Hayek, M., Restrepo-Coupe, N., Wiedemann, K. T., Xu, X., Wehr, R., Christoffersen, B. O., Miao, G., Da Silva, R., et al.: Partitioning controls on Amazon forest photosynthesis between environmental and biotic factors at hourly to interannual timescales, Global Change Biology, 23, 1240–1257, 2017.

Yan, Y., Klosterhalfen, A., Moyano, F., Cuntz, M., Manning, A. C., and Knohl, A.: A modeling approach to investigate drivers, variability and uncertainties in O_2 fluxes and O_2: CO_2 exchange ratios in a temperate forest, Biogeosciences, 20, 4087–4107, 2023.

Yeager, S. G., Rosenbloom, N., Glanville, A. A., Wu, X., Simpson, I., Li, H., Molina, M. J., Krumhardt, K., Mogen, S., Lindsay, K., et al.: The seasonal-to-multiyear large ensemble (SMYLE) prediction system using the Community Earth System Model version 2, Geoscientific Model Development, 15, 6451–6493, 2022.

Zhalnina, K., Louie, K. B., Hao, Z., Mansoori, N., Da Rocha, U. N., Shi, S., Cho, H., Karaoz, U., Loqué, D., Bowen, B. P., et al.: Dynamic root exudate chemistry and microbial substrate preferences drive patterns in rhizosphere microbial community assembly, Nature microbiology, 3, 470–480, 2018.